NAVAL POSTGRADUATE SCHOOL

MONTEREY, CALIFORNIA

THESIS

CONCEPTUAL AND PRELIMINARY DESIGN OF A LOW-COST PRECISION AERIAL DELIVERY SYSTEM

by

Andrew B. Hall

June 2016

Thesis Advisor: Oleg A. Yakimenko
Second Reader: Fotis A. Papoulias

Approved for public release; distribution is unlimited

THIS PAGE INTENTIONALLY LEFT BLANK

REPORT DOCUMENTATION PAGE			Form Approved OMB No. 0704–0188
Public reporting burden for this collection of information is estimated to average 1 hour per response, including the time for reviewing instruction, searching existing data sources, gathering and maintaining the data needed, and completing and reviewing the collection of information. Send comments regarding this burden estimate or any other aspect of this collection of information, including suggestions for reducing this burden, to Washington headquarters Services, Directorate for Information Operations and Reports, 1215 Jefferson Davis Highway, Suite 1204, Arlington, VA 22202-4302, and to the Office of Management and Budget, Paperwork Reduction Project (0704-0188) Washington, DC 20503.			
1. AGENCY USE ONLY ***(Leave blank)***	**2. REPORT DATE** June 2016	**3. REPORT TYPE AND DATES COVERED** Master's Thesis	
4. TITLE AND SUBTITLE CONCEPTUAL AND PRELIMINARY DESIGN OF A LOW-COST PRECISION AERIAL DELIVERY SYSTEM			**5. FUNDING NUMBERS**
6. AUTHOR(S) Andrew B. Hall			
7. PERFORMING ORGANIZATION NAME(S) AND ADDRESS(ES) Naval Postgraduate School Monterey, CA 93943-5000			**8. PERFORMING ORGANIZATION REPORT NUMBER**
9. SPONSORING /MONITORING AGENCY NAME(S) AND ADDRESS(ES) N/A			**10. SPONSORING / MONITORING AGENCY REPORT NUMBER**
11. SUPPLEMENTARY NOTES The views expressed in this thesis are those of the author and do not reflect the official policy or position of the Department of Defense or the U.S. Government. IRB Protocol number ____N/A____.			
12a. DISTRIBUTION / AVAILABILITY STATEMENT Approved for public release;distribution is unlimited			**12b. DISTRIBUTION CODE**

13. ABSTRACT (maximum 200 words)

The Army and Air Force have interest in the development of a Joint Precision Aerial Delivery System (JPADS) that could remotely and accurately resupply dispersed and geographically isolated ground forces. The Marine Corps has requested options that offer increased accuracy, lighter payloads, greater stand-off distances and reduced cost. To date, most research has resulted in a series of large, expensive and platform-specific solutions, which do not capitalize on the enhanced range and capability afforded by existing and commercially available unmanned aerial system technology. The systems engineering processes contained in the conceptual and preliminary design phases are utilized to investigate and develop a potentially low-cost alternative to existing systems. Using an Agile methodology, individual components are designed and incorporated into an integrated aerial system that utilizes an autonomously guided and controlled ram-air parachute delivered from an unmanned aerial platform. Employment of the low-cost micro-light weight class of JPADS has the potential to provide all services with a near-term platform to remotely deliver diverse logistical and sensor payloads while minimizing risk to forces.

14. SUBJECT TERMS conceptual design, preliminary design, Agile methodology, autonomous navigation, precision aerial delivery, parachute, control			**15. NUMBER OF PAGES** 118
			16. PRICE CODE
17. SECURITY CLASSIFICATION OF REPORT Unclassified	**18. SECURITY CLASSIFICATION OF THIS PAGE** Unclassified	**19. SECURITY CLASSIFICATION OF ABSTRACT** Unclassified	**20. LIMITATION OF ABSTRACT** UU

NSN 7540–01-280-5500 Standard Form 298 (Rev. 2–89)
Prescribed by ANSI Std. 239–18

THIS PAGE INTENTIONALLY LEFT BLANK

Approved for public release; distribution is unlimited

CONCEPTUAL AND PRELIMINARY DESIGN OF A LOW-COST PRECISION AERIAL DELIVERY SYSTEM

Andrew B. Hall
Commander, United States Navy
B.S., United States Naval Academy, 1999

Submitted in partial fulfillment of the
requirements for the degree of

MASTER OF SCIENCE IN SYSTEMS ENGINEERING

from the

NAVAL POSTGRADUATE SCHOOL
June 2016

Approved by: Oleg A. Yakimenko
Thesis Advisor

Fotis A. Papoulias
Second Reader

Ronald E. Giachetti
Chair, Department of Systems Engineering

THIS PAGE INTENTIONALLY LEFT BLANK

ABSTRACT

The Army and Air Force have interest in the development of a Joint Precision Aerial Delivery System (JPADS) that could remotely and accurately resupply dispersed and geographically isolated ground forces. The Marine Corps has requested options that offer increased accuracy, lighter payloads, greater stand-off distances and reduced cost. To date, most research has resulted in a series of large, expensive and platform-specific solutions, which do not capitalize on the enhanced range and capability afforded by existing and commercially available unmanned aerial system technology. The systems engineering processes contained in the conceptual and preliminary design phases are utilized to investigate and develop a potentially low-cost alternative to existing systems. Using an Agile methodology, individual components are designed and incorporated into an integrated aerial system that utilizes an autonomously guided and controlled ram-air parachute delivered from an unmanned aerial platform. Employment of the low-cost micro-light weight class of JPADS has the potential to provide all services with a near-term platform to remotely deliver diverse logistical and sensor payloads while minimizing risk to forces.

THIS PAGE INTENTIONALLY LEFT BLANK

TABLE OF CONTENTS

THIS PAGE INTENTIONALLY LEFT BLANK

LIST OF FIGURES

THIS PAGE INTENTIONALLY LEFT BLANK

LIST OF TABLES

THIS PAGE INTENTIONALLY LEFT BLANK

LIST OF ACRONYMS AND ABBREVIATIONS

AACUS	Autonomous Aerial Cargo/Utility System
AADS	autonomous aerial delivery system
ADS	aerial delivery system
ADSC	Aerodynamic Deceleration Systems Center
AGL	above ground level
AGU	airborne guidance unit
ARC	air release circle
ARP	air release point
BEC	battery eliminator circuit
CARP	calculated air release point
COI	critical operational issue
CONOPS	concept of operations
COTS	commercial-off-the-shelf
DOD	Department of Defense
DODAF	Department of Defense architecture framework
DZ	drop zone
FOB	forward operating base
GPS	global positioning system
GUI	graphical user interface
IED	improvised explosive device
INP	innovative naval prototype
INS	inertial navigation system
IP	impact point
JMUA	Joint Military Utility Assessment
JPADS	Joint Precision Air Drop System
JTF	Joint Task Force
MCCS	mission command and control center
MEDEVAC	medical evacuation
MIMO	multiple input multiple output
MOE	measure of effectiveness

MOP	measure of performance
NGO	non-governmental organization
NPS	Naval Postgraduate School
ONR	Office of Naval Research
OV	operational view
PAD	precision aerial delivery
PADS	precision aerial delivery system
PI	point of impact
POI	point of landing
SOCOM	Special Operations Command
SISO	single input single output
UAS	unmanned aerial system
UAV	unmanned aerial vehicle
UKF	unscented Kalman filter
USMC	United States Marine Corps
VTOL	vertical takeoff and landing

EXECUTIVE SUMMARY

Aerial delivery systems (ADSs) have a well-documented history of affecting the military battlefield at both the strategic and operational levels for the better part of the last century, and recent technological advances have facilitated an extraordinary increase in the precision and accuracy of these systems. The range of payload sizes and weights has continued to expand, as have demands for increased accuracy and reliability associated with delivery. Technological advancements in ram-air parachute design, unmanned aerial vehicles (UAVs) and inertial navigation systems (INSs) continue to generate expanded interest by the United States Marine Corps (USMC) in bringing smaller payload sizes, and their associated capabilities, to the modern tactical battlefield. This research applies a systems engineering approach to design a prototype micro-light weight class precision aerial delivery system (PADS) to determine whether low-cost, commercial-off-the-shelf (COTS) navigation components can provide sufficient accuracy and reliability to close the capability gap between the systems currently in operation and the combat operational need for rapid-response, tactical logistical resupply in austere and dispersed locations.

In order to address the primary research question, a brief summary on the history of PADSs and descriptions of the general classes are included. The aerodynamic fundamentals of ram air parachutes are briefly discussed, and an introduction to the terminology used in the development and testing of PADSs is provided. Previous Naval Postgraduate School (NPS) research in the development of the Blizzard autonomous aerial delivery system (AADS), as well as methods for updating and enhancing PADS navigational accuracy are presented. The standard measures of performance (MOPs) and measures of effectiveness (MOEs) used for the development of PADSs are described, as well as the application of the Agile methodology in systems engineering. Several potential additional PADS mission areas also are summarized.

The application of traditional and Agile system engineering methodologies is explained, including the various technical activities associated with the conceptual and preliminary design phases. The core problem that PADSs are designed to resolve is

identified, and subsequently, the basic PADS functions are listed for both operational and experimental settings. The needs, wants and concerns of several stakeholders are detailed, as well as the design criteria that influenced conceptual design. Points of contrast between operational and experimental system design criteria are highlighted. Several architecture decisions are described including the influence of shifting design considerations on the architectural evolution. The operational concept for employment of PADSs is discussed and a functional analysis is specified.

Subsequently, the conceptual and preliminary design of a Snowflake ADS and several additional components of the Blizzard AADS are described. The specifications for the two types of UAVs that were utilized in flight-testing are included. Several iterations and a final prototype design are summarized, including the installation and usage of two types of commercial-off-the-shelf (COTS) available autopilot computers. A description of the final design for a power distribution sub-system is detailed, as early iterations contributed to unexpected failures in testing and experimentation. A description of each type of ram air parachute is included, as well as the three types of UAV/Snowflake separation sequences. A comparison between the flight control dynamics of fixed-wing platforms and a ram air parachute platform is incorporated, as it proved to be a significant challenge in the implementation of COTS technology.

A comprehensive summary of 65 flight tests over a nearly ten-month period, and several simulations conducted in the Aerodynamic Deceleration Systems Center (ADSC) laboratory at NPS are included. The results from the flight tests are correlated with sequential improvements in the parachute deployment methods that were derived from failure mode analysis. Additionally, the ability of each autopilot to capture and retain valid experimental data is described, as it directly influenced the author's conversion from the original flight computer to a second type. Various lab simulations and the mathematics used to convert recorded data to a more useful coordinate frame using quaternions are detailed. Subsequently, a representative flight profile is described and illustrated to facilitate follow-on control system development.

In summary, the application of systems engineering methodology to influence conceptual and preliminary design is described in detail and utilized throughout prototype design. While full operational capability was not realized during the course of this research, several conclusions were identified, including the potential for follow-on improvements in design. Low-cost, COTS navigation components are likely to provide sufficient accuracy and reliability to close the capability gap between the PADSs currently in operation and the combat operational need for rapid-response, tactical logistical resupply in austere and dispersed locations. However, continued research is warranted to determine whether performance and reliability requirements can be delivered in a low-cost manner.

THIS PAGE INTENTIONALLY LEFT BLANK

ACKNOWLEDGMENTS

I would like to thank Professor Oleg Yakimenko for his enthusiasm, advice, and mentorship during the last two years, and for the opportunity to practice hands-on engineering and field experimentation. I feel fortunate to have had the opportunity to learn from him. I also want to acknowledge the support of Professor Fotis Papoulias; without him, this research would not have been possible. I am indebted to Matt O'Brian and Alan Stephens; their insights and humor made working through challenges a pleasure. Most significantly, I want to recognize Sarah, Elizabeth and Ethan for their patience and support. I never would have gotten here without them.

THIS PAGE INTENTIONALLY LEFT BLANK

I. INTRODUCTION

A. BACKGROUND

Aerial delivery systems (ADSs) have a well-documented history of affecting the military battlefield at both the strategic and operational levels for the better part of the last century, and recent technological advances have facilitated an extraordinary increase in the precision and accuracy of these systems. The range of payload sizes and weights has continued to expand, as have demands for increased accuracy and reliability associated with delivery. Early precision aerial delivery systems (PADSs) were designed and constructed to deliver large payloads for strategic and operational logistical resupply with a predetermined accuracy specification. The United States Marine Corps (USMC) has stated that "expanded use of unmanned systems for resupply of forward-based units is not only viable, it is a critical operational requirement" (United States Marine Corps [USMC] 2013, 28). Technological advancements in ram-air parachute design, unmanned aerial vehicles (UAV) and inertial navigation systems (INSs) continue to generate expanded interest by the USMC in bringing smaller payload sizes, and their associated capabilities, to the modern tactical battlefield.

In response to a current warfighting capability gap in the ability to provide tactical logistical support while minimizing risk to forces, the Office of Naval Research (ONR) has developed the Autonomous Aerial Cargo/Utility System (AACUS) Innovative Naval Prototype (INP) Concept of Operations (CONOPS) with the goal of providing rapid-response payload delivery by utilizing advanced autonomous capabilities. ONR expected that developed systems should be able to take advantage of unmanned vertical takeoff and landing (VTOL) capabilities and provide reliable delivery of medical and logistical supplies to geographically dispersed units in austere locations and environments. The AACUS INP CONOPS also includes the additional complexity of landing area obstacle detection and avoidance, and autonomous landing at unprepared landing sites and the ability for terminal users to execute supervisory control without specialized training (Office of Naval Research [ONR] 2012, 2).

Advances in PADSs have potentially merged with the capability shortfalls highlighted in the AACUS INP CONOPS and offer a potentially simpler and less expensive solution than some of the technologies and solutions envisioned by ONR. Focused systems engineering research is warranted in the design and applicability of ultra-light PADSs as a potential solution. PADSs have the potential to offer fewer complications, reduce exposure to hostile threat, lower cost, and increase range and endurance capability. The capability gap summarized by ONR, has been expressed by numerous Department of Defense (DOD) entities and can potentially be closed with the use of PADSs for significantly lower costs in terms of both financial resources and technical complexity.

B. OBJECTIVES

The primary objective of this thesis is to utilize a systems engineering approach to design a prototype micro-light weight class PADS and to answer the following question:

- Can low-cost, commercial-off-the-shelf (COTS) navigation components provide sufficient accuracy and reliability to close the capability gap between the systems currently in operation and the combat operational need for rapid-response, tactical logistical resupply in austere and dispersed locations?

Additionally, secondary research questions are

- What are the operational limitations for employing a micro-light weight class PADS?
- Can various systems engineering methodologies be applied to a research area to provide insight and improved functionality during conceptual and preliminary design?
- What are the key differences between a prototype design constructed for operational use as compared to a design constructed to support scientific experimentation?
- Does the NPS Systems Engineering curriculum adequately prepare its students to work within a multi-discipline engineering team to complete a technical thesis, including prototype design, construction and field experimentation?

C. RESEARCH

Preliminary research was conducted utilizing open source government documentation, discussions with unmanned aerial systems (UAS) and PADS subject matter experts, laboratory experimentation and field flight experimentation at McMillan Airfield, Camp Roberts, CA.

The following computational and electronic resources were utilized during various phases of this research:

- **APM Planner 2.0**: Open source application for configuring, testing and calibrating autonomous vehicle control platforms. Specifically, APM Planner 2.0 was used with the Pixhawk autopilot in early research and flight-testing.
- **Rowley CrossWorks for ARM Version 3**: Comprehensive C/C++ assembly language development system used for programming, compiling and debugging an X-Monkey autopilot.
- **MATLAB 2015B:** A high-level language and computational software tool used extensively for data analysis of flight parameters and control system design.

D. CURRENT STATE

The Snowflake ADS, an ongoing research project at the Naval Postgraduate School (NPS), started in 2008 and utilizes a series of commercially available sensors that integrate data from global positioning systems, three axis accelerometers, three axis gyros, a magnetometer and a barometric altimeter. The previous guidance design utilized a series of highly developed and specific algorithms that facilitated the guidance and control of a two skin rectangular parafoil. Various parafoils could be attached to the Snowflake system to facilitate payloads of different sizes. Unfortunately, a good portion of the resident Snowflake experts had departed NPS, and a significant number of the components required for ongoing experimentation were no longer available.

1. Capabilities Gap

The ONR CONOPS highlights the following two capability shortfalls:

> Executing resupply is significantly challenging due to primarily the lack of paved roads coupled with difficult, mountainous terrain which has diminished the effectiveness of traditional means of overland logistics movement using ground transportation. The Joint Force needs an alternate means to provide sustained, time sensitive, logistics support over widely dispersed locations.
>
> Combat in urban environments has shown that moving a casualty can be difficult and time consuming. Moving an individual only a few hundred yards can take an hour or more. The extended lines of communication between forces and their forward operating bases (FOBs) (inclusive of Medical Evacuation (MEDEVAC) by aircraft) are at risk of enemy ambush or improvised explosive device (IED) attack (ONR 2012, 3).

The USMC also has requested research and investment in the usage of unmanned transportation systems and robotic systems to assist with resupply to the engaged warfighter. The goal is tailored delivery while minimizing risk to human life. (USMC 2013, 30) In general, the USMC has viewed previously developed JPADSs as being too large, too heavy, too expensive and not responsive enough to urgent warfighter needs.

2. Constraints

The principal constraint of an updated Snowflake ADS is that it must be designed to close the current capability gap (or at least a portion of it) to offer increased simplicity, reduced exposure to hostile threat and/or reduced cost. The capability gaps described do not need to be met in their entirety. As such, PADSs that can close one of the capability gaps with significantly enhanced simplicity should not be excluded from consideration simply because it does not perform both. The ONR CONOPS indirectly advocates for a solution that can be terminally controlled as well as landed and re-launched in the field. The updated Snowflake ADS must be able to accomplish the intended delivery requirement, and if it can sufficiently deliver payload via autonomous parachute, then the complexity of landing and relaunching can be avoided.

E. DESIRED STATE

The desired capability resulting from this research is a systems engineering approach to conceptual and initial design of a Snowflake ADS to perform small-scale logistical resupply in a more efficient manner than existing systems do. The research is

designed to examine the capability gaps closely, analyze the effective stakeholder needs and design a potential solution to achieve the objective economically.

F. METHODOLOGY

This research was conducted in parallel with the effort of Lieutenant Commander Matthew O'Brian, from the Naval Postgraduate School (NPS) Undersea Warfare Curriculum. As Lieutenant Commander O'Brian conducts research in support of the Dynamic Systems and Control Track in the Mechanical Engineering Department, the author intended to pair with O'Brian's research effort by applying a systems engineering methodology to maintain a direct link between the research being conducted and resolution of a stakeholder need or requirement. Utilizing cross-domain and multi-field engineering principles, the author integrated multiple components and disciplines ranging from computer programming, electrical engineering, radio frequency communication, classic control and aerodynamics. The author's intent was to conceptually and preliminarily design and engineer a complete logistical delivery system which could be used to contribute to the battlefield.

To assist in accomplishing the design and engineering, the author used a hybrid systems engineering and analysis approach, with substantial input from Blanchard and Fabrycky, as well as an Agile systems engineering methodology used within the PADS industry for the design and engineering phases. The Blanchard and Fabrycky methods were used to correlate effectively the stakeholder needs from operational users and to develop an updated design of the Snowflake ADS while providing traceability. The author also used elements of the Agile methodology and design thinking principles to provide targeted iteration within the conceptual and initial design phases.

Though the parallel effort of Lieutenant Commander O'Brian is focused on the classical and modern methods of control associated with guidance and navigation of the Snowflake ADS, the concepts have been incorporated from conceptual design. The Snowflake ADS was designed to capture sufficient data and serve as a platform for experimentation to support the development of the various plant models required for effective feedback control.

G. THESIS ORGANIZATION

To address the objectives and research questions detailed in section B, this thesis is arranged as follows:

- Chapter II presents a summary of related work. It includes a brief history on the development, classification and utility of Joint Precision Air Drop Systems (JPADSs), the fundamentals of a ram-air parachute, the fundamentals of aerial delivery systems, a description of the Blizzard autonomous aerial delivery system (AADS), a summary of two techniques used to enhance terminal accuracy, a description of measures of effectiveness (MOEs) and measures of performance (MOPs) used to assess PADSs and an overview of the Agile methodology as applied to systems engineering a PADS

- The application of systems engineering methodology is covered in Chapter III. It includes an overview of conceptual and preliminary design, the problem definition and needs identification, a stakeholder analysis, design criteria used, the operational concept for PADSs and a functional analysis

- Chapter IV details the design of the Snowflake system components. It includes a description of the Arcturus T-20 and JUMP 20 UAVs, overview of the Snowflake ADS including the design of the autonomous guidance unit (AGU), specifications of the ram-air parachutes used, summary of the various parachute deployment sequences and a description of the flight control dynamics associated with ram air parachute control

- Chapter V compiles the Snowflake simulation and test results. It includes an analysis of the failure modes encountered during flight experimentation, methodology used for conducting coordinate transformation and analysis of representative flight test results

- This thesis ends with Chapter VI, which provides a conclusions and series of recommendations. It includes an assessment of the incorporation of low-cost technology in the development of a micro-light weight class PADS, discussion of the associated operational employment limitations, description of the utility of systems engineering methodologies utilized in conceptual and preliminary design as well as several technical recommendations for potential improvements to the Snowflake ADS.

In summary, PADSs have been present on the military battlefield for an extended period and have been asked to perform traditional logistical supply missions. As warfare has evolved, the services have requested PADSs with expanded mission capability through increased accuracy, decreased size, longer stand-off ranges and reduced cost.

This chapter articulates the primary objective of this thesis, as well as secondary research questions that were examined in the course of research and experimentation. Additionally, the current and desired end state of the research is addressed. Finally, this chapter outlines the methodology used and organization of the thesis to assist the reader.

THIS PAGE INTENTIONALLY LEFT BLANK

II. RELATED WORK

A. PREVIOUS RESEARCH

A significant amount of research has been conducted over the previous 50 years in the field of precision aerial delivery, driven largely by advances in controlled gliding ram-air parachutes as compared to the uncontrolled round parachutes that preceded (Yakimenko 2015,1). Driven by the desire to deliver logistics remotely with increased accuracy, dozens of PADSs have been developed, each designed to deliver a diverse series of payload sizes. Additionally, new applications have continually been examined (Yakimenko 2015, 1). The following summary of related works includes the history and development of JPADSs, a basic analysis of a ram-air parachute, a description of a previous NPS research endeavor to field an AADS, a series of estimation techniques used to refine landing accuracy, a proposed set of MOEs and MOPs used to evaluate PADS effectiveness and a description of a systems engineering methodology used to develop and field a representative PADS.

B. JPADS PROGRAM

The Joint Precision Air Drop System (JPADS) was a United States (U.S.) Army/U.S. Air Force program jointly developed to examine potential accuracy improvements. The goal of the JPADS program was to develop the capability to deliver air cargo anywhere in the world within 24 hours. The U.S. Air Force research effort focused on the development of a mission planning system that could aggregate available wind data over a drop zone (DZ), forecast expected wind and calculate a calculated air release point (CARP). This release point should minimize the landing error of a conventional unguided aerial delivery system (ADS) (Yakimenko 2015, 10).

In conjunction with the mission planning system, the U.S Army concurrently expended research effort to develop a series of AGUs as well as representative systems in the classes that evolved to those indicated in Table 1.

Table 1. JPADS Categories. Adapted from *Defense Industry Daily* (2016).

JPADS Weight Class	Weight Range
Micro-light weight (ML)	~5-70 kg (10-150 lb)
Ultra-light weight	~100-300 kg (250-700 lb)
Extra-light weight (XL)	~300 kg-1.1 tons (700-2,400 lb)
Light weight (L)	~2.3-4.5 tons (5,000-10,000 lb)
Medium weight (M)	~4.5-19 tons (10,000-42,000 lb)

In addition to simple logistical delivery, the technology developed though the JPADS program has proposed applicability that extends well beyond resupply. In his 2015 summary of the JPADS program, Yakimenko proposes the following additional military and security applications:

- Provide accurate and flexible stealth supply to special forces teams.
- Provide navigational guide for team night insertion.
- Support pathfinder operation.
- Deploy acoustic sensing equipment into battlefield.
- Deploy electronic warfare equipment.
- Deliver leaflets accurately.
- Deploy nuclear, biological and chemical threat sensors.
- Provide “just in time” supply of advancing troops (2015, 10–1)

Additionally, Yakimenko also proposes that PADS capabilities can extend well beyond military applications to provide:

- space items recovery (as a final stage of a multistage system)
- regular supply of remote locations

- humanitarian aid and disaster relief deployment to inaccessible locations and unprepared DZs including potential field hospitals, refugee camps and United Nations compounds
- all-weather equipment drop for search and rescue operations
- equipment supply to first responders in disaster areas
- equipment delivery into rugged mountain areas
- sensing equipment and video/radio uplink deployment
- medical equipment supply
- precision delivery of buoys and lifeboats at sea (2015, 11)

C. FUNDAMENTALS OF RAM-AIR PARACHUTES

In 2015, Steven Lingard presented an updated summary on the fundamental design of a ram-air parachute. Lingard stated (2015, 73–4) that the ram-air parachute, or parafoil, was developed in the early 1960s with the effective design replicating a low-aspect wing, constructed entirely with fabric without any rigid supporting structure. Additionally, Lingard notes that flexibility inherent in a fabric design facilitated packing and airborne deployment, similar to previous drag parachute designs, though the airfoil characteristics were more closely related to wings than to basic drag parachutes. When viewed from above or below, a basic parafoil has a rectangular shape, but the cross section is a series of individual airfoils. The upper surface of the parafoil is joined to the bottom surface of the parafoil by a series of flexible fabric ribs, which form cells as shown in Figure 1. Lingard added that the leading edge of the wing is kept open to allow air to enter and fill the parafoil, yet the trailing edge is sealed to retain inflation. There is typically a series of apertures cut into the ribs to facilitate the flow of air between cells during inflation and the equalization of pressure between cells once the parafoil is inflated.

Lingard continues (2015, 74) that to preserve the basic airfoil shape in the bottom surface, there is a series of suspension lines fastened at various intervals along the ribs between cells. A rib with suspension lines becomes a loaded rib, and a non-loaded rib is one without suspension lines. Non-loaded ribs serve to separate each parafoil cell into

semi-cells as shown in Figure 1. These suspension lines are typically cascaded into primary suspension lines to reduce the overall drag for the parafoil system. Stabilizer panels can be added to the edges of the parafoil to assist in directional stability by channeling the flow of air along the parafoil rather than around the wingtip which creates a more unpredictable vortex.

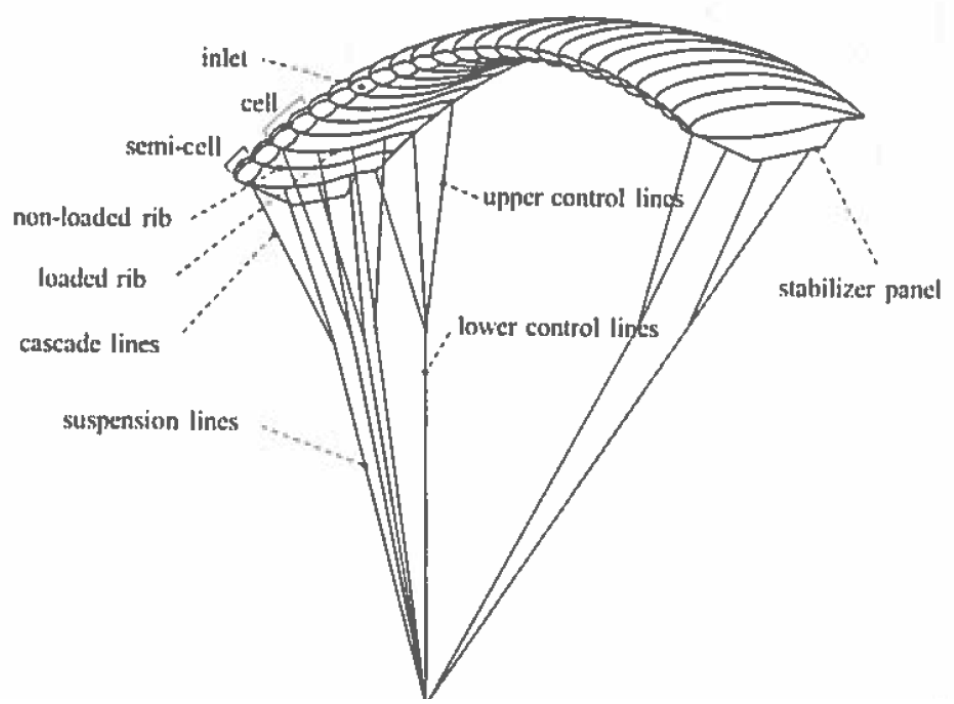

Figure 1. Basic Ram-Air Parachute. Source: Lingard (2015).

Unfortunately, the drag associated with the suspension lines becomes a significant factor as the size of the parafoil is increased. As a result, the drag of the parafoil cannot be considered by itself. Instead, a systems perspective is needed, where parafoil drag is one contributor to the overall system, which also includes the drag of the suspension lines. In order to preserve the basic flying qualities of the parafoil and to reduce the length of the suspension lines, the ram-air wing is given an arc anhedral, which is also referred to as the crown rigging (2015, 84). The amount of anhedral (ε) is a function of the line length (R) and the span of the parafoil (b). The comparison between the dihedral angle of a conventional wing and the anhedral angle of a ram-air wing is shown in Figure 2.

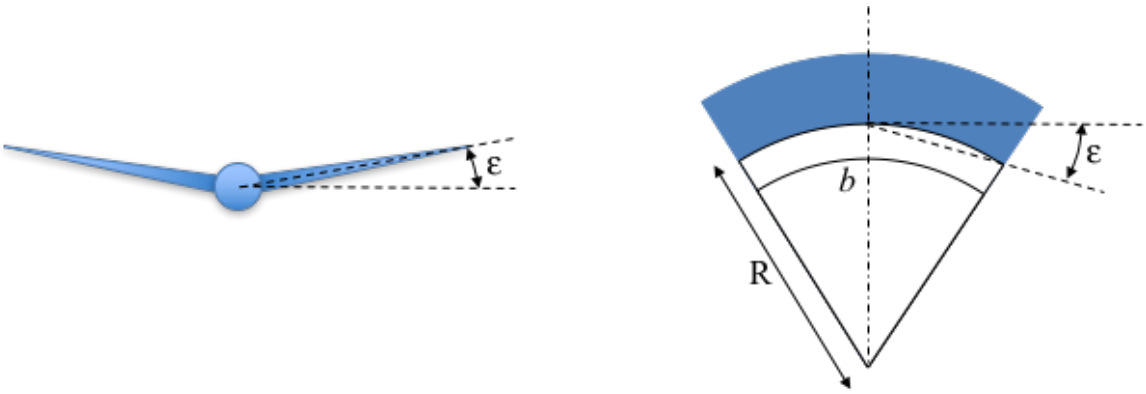

Figure 2. Contrast of Conventional Wing Dihehdral and Ram-Air Wing Anhedral. Adapted from Lingard (2015).

Lingard (2015, 92) also proposes the following model to simplify the basic forces acting on a parafoil system in flight. The free body diagram shown in Figure 3 graphically describes the relationship of the various forces acting on the components of the parafoil system. In this diagram, each component has a drag, lift and weight force, with the exception of the suspension line weight, which is considered negligible. The velocity shown (V) represents velocity through the air mass. Obviously, taking dynamically changing wind velocity into account creates a much more complex series of relationships. The glide angle (γ) is the angle between the parafoil velocity vector and the horizontal as show in Figure 3.

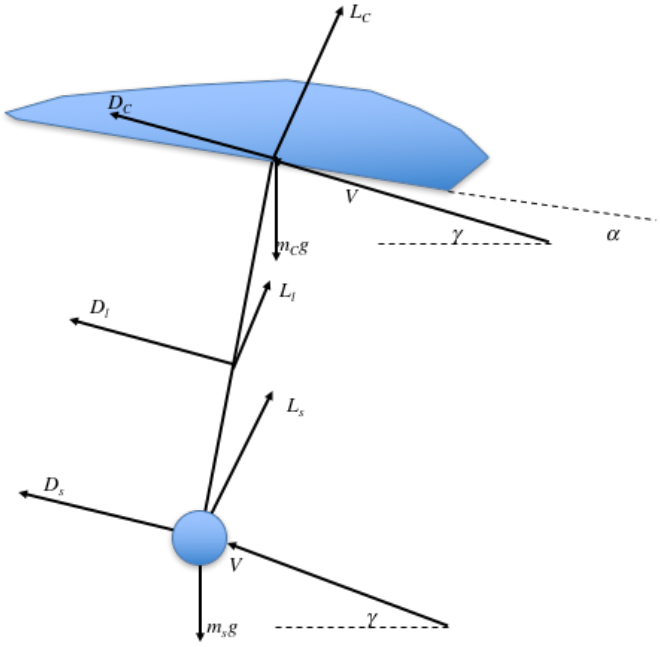

Figure 3. Ram-Air Parachute in Steady State Gliding Flight. Adapted from Lingard (2015).

To maintain effective lateral control of a ram-air parachute, Lingard (2015, 119) described the concept of trailing edge deflection with some relative approximations for the yawing moment that could be generated by asymmetric trailing edge deflection. The yaw rate, in radians per second, can be determined using the following expression:

$$r = 0.71\frac{V}{b}\delta_a$$

where V denotes the airspeed, b denotes the span of the ram-air parachute and δ_a denotes the amount of asymmetric trailing edge deflection in radians per second.

D. FUNDAMENTALS OF AERIAL DELIVERY SYSTEMS

To standardize the relationships between various factors considered during the execution of a precision aerial delivery (PAD) mission, Brown and Benney (2005, 4) defined the following terms, each of which is illustrated in Figure 4:

- Impact point (IP): designated point of intended landing
- Point of impact (PI): actual point of landing

- Air release point (ARP): point of release of the airdrop unit from the drop aircraft
- Ballistic trajectory: trajectory along which an unguided, drag-only body would fall in order to reach the IP
- Ballistic ARP: the intersection of the delivery aircraft flight path with the ballistic trajectory, i.e., a theoretically perfect release point
- CARP: Standard airdrop terminology for the calculated location of the ARP based on estimated winds
- Air release circle (ARC): a circle at the release altitude, centered on the Ballistic ARP, within the glide performance of the system is sufficient to reach the IP.

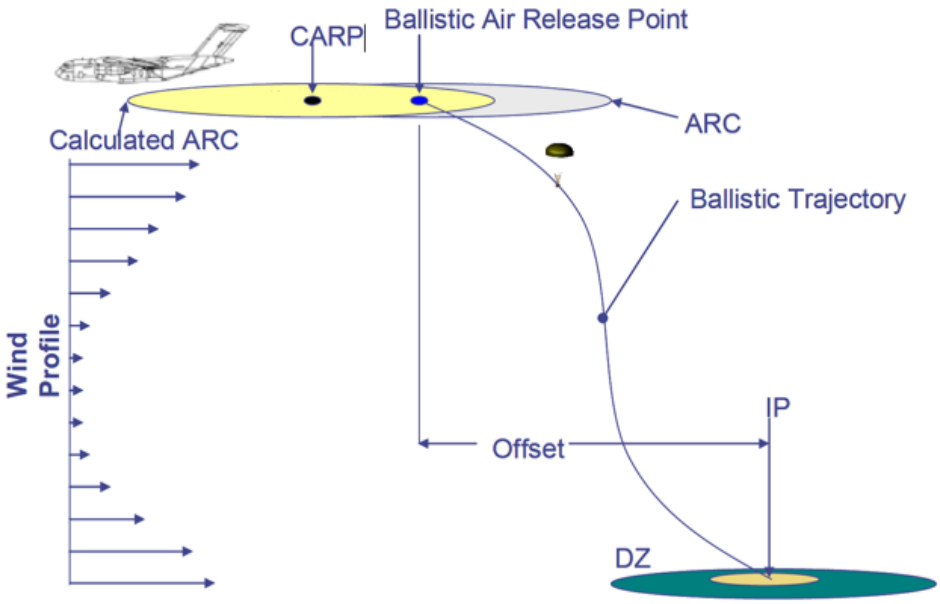

Figure 4. Terms Associated with Aerial Delivery Systems. Source: Brown and Benney (2005).

The location of the CARP becomes significant when the wind estimation contains error, which is likely, or when there are multiple drops intended for the same IPs. To ensure safe separation of PADSs, the delivering platform will incorporate some time between successive PADS release, which will correspond to a positional displacement requiring compensation during the PADS's flight and navigation profile.

E. BLIZZARD AADS

In 2008, a coordinated effort between U.S. Special Operations Command (SOCOM) and the NPS Aerodynamic Deceleration Systems Center (ADSC) conducted research to design a system for ultra-light-weight precision aerial delivery. Researchers from NPS and the University of Alabama presented a miniature prototype, termed the Blizzard AADS, which utilized an inertial trajectory and an estimate of surface winds to compute a final standard-approach-pattern and landing maneuver into the wind. Accuracy results from the Blizzard AADS were inside of 10m CEP (Yakimenko et al. 2011, 1–2).

The Blizzard AADS consisted of a four major components: the T-20 unmanned aerial vehicle, the Snowflake ADS, a ground mission command and control center (MCCC), and an optional ground target weather station. The MCCC facilitated the entry of target coordinates; the weather station allowed updated target area winds to be used for landing accuracy improvements and the T-20 delivered the payload to a pre-determined launch location. The Snowflake ADS was a small 4”x8”x10” payload container consisting of avionics and control actuators, including a global positioning system (GPS) receiver, three-axis accelerometers, gyroscopes, a magnetometer and a barometric altimeter (Yakimenko et al. 2011, 2–4).

The Blizzard AADS proved to be a nearly complete fielded system, useful for follow-on research and concept exploration. The research proved the accuracy of the system and showed that enhancements and subsequent examination of additional applications were possible.

F. POSE ESTIMATION AND MONOCULAR AUGMENTATION

In his Ph.D. dissertation, Hewgley (2014, v) provides two methods to aid in enhancing PADS accuracy. In an effort to better estimate the winds between a descending ADS and the intended point of landing (POI), Hewgley assumes a logarithmic relationship between the air mass height and the horizontal wind velocity. The estimation technique facilitates a better estimation of the PADS’s computation of terminal winds and the computation of a landing trajectory.

Utilizing the previously described Snowflake ADS as an experimentation platform, Hewgley developed a method wherein the Snowflake measured real-time wind speed and direction aloft, utilized a logarithmic model of boundary layer winds near the surface and continually computed the wind direction and speed that it would fall through during the remainder of the descent. This method, summarized in Figure 5, was particularly suited for shipboard and maritime usage in which the course and speed of the ship can be adjusted to produce a relatively predictable wind (Hewgley 2014, xxiii).

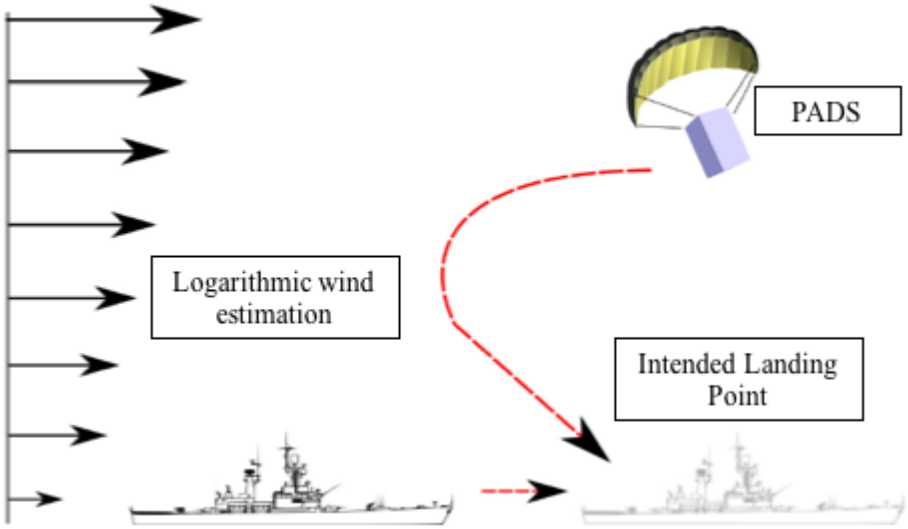

Figure 5. Logarithmic Wing Estimation Used for Planning Intended Landing Point. Adapted from Hewgley (2014).

Additionally, to assist in target motion estimation, Hewgley opted to utilize a monocular vision camera. The monocular system was selected for simplicity and a cost reduction. By using a simple geometric projection, a homogeneous coordinate transformation and a subsequent state-space formulation, the Snowflake ADS utilized its monocular sensor to provide navigation adjustments based on relative motion between the sensor and the target (Hewgley 2014, 45). Additionally, Hewgley provides an unscented Kalman filter (UKF) algorithm to blend the target in-target and out-of-target measurement error covariance matrices as a monocular sensor is unlikely to retain the

target within view due to the pendulum oscillations caused by the descending ram-air parachute (Hewgley 2014, 90–91).

G. MEASURES OF PERFORMANCE AND EFFECTIVNESS

Three critical operational issues (COIs) were created to guide the development of JPADSs in the mid-2000s, which were subsequently used during a Joint Military Utility Assessment (JMUA) of existing technologies. They were

- COI 1. Does the JPADS system-of-systems successfully support payload delivery at the target weights and standoff distances in its intended operational environment?
- COI 2. Does the JPADS system-of-systems provide the Joint Task Force (JTF) Commander with an enhanced operational capability?
- COI 3. Is the JPADS system-of-systems suitable for employment in its intended environments? (Benney et al. 2005a, 11)

1. System Reliability and Accuracy

PADS accuracy was described in detail by Brown and Benney (2005, 3). System reliability was defined as the probability of a PADS successfully reaching a location near the DZ from which a successful guided approach and landing at the intended IP could be achieved. Terminal accuracy was the distance from IP to the nearest of all landing points that fall within a specified probability level. Overall system accuracy was defined as the distance from the IP to the nearest of all landing points landing within a specified probability level. These relationships are summarized in Figure 6, with the significant distinction that an unreliable system is still characterized as a valid, though inaccurate system.

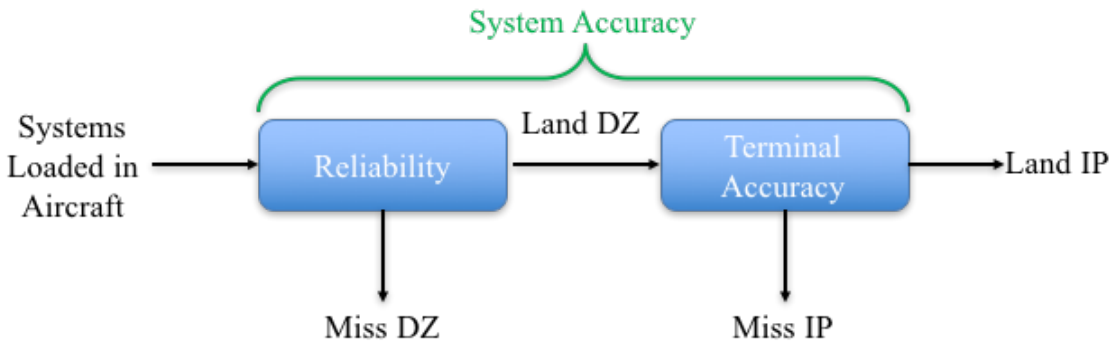

Figure 6. Relationship Between System Accuracy, Reliability and Terminal Accuracy. Adapted from Brown and Benney (2005).

2. Reliability: Failure Modes and Effects

In 2015, expanding the definitions set by Brown and Benney, Yakimenko characterized five potential failure modes that could affect the reliability of the PADS as follows:

- air carrier missing CARP (which is especially critical for unguided ADSs or PADSs with very limited control authority)
- parachute failure to open (can include several submodes depending on the number of PADS stages)
- parachute or control line damage
- failure of the AGU to operate properly
- excessive actual winds aloft (compared to predicted) precluding reaching the DZ even if everything works correctly (2015, 14)

H. AGILE METHODOLOGY

In addition to simply developing and advancing the capabilities of PADSs, significant advances have been made in the utilization of Agile development methodologies and their utility in executing systems engineering through the development of parachute systems. In 2011, Barber et al. discussed their use of an Agile methodology as an alternative to the conventional Plan Driven Product Development Life cycles (PD-PDLC), or "waterfall" development shown in Figure 7. They advocated the three essential Agile values that made it unique:

- Requirements are too important to be left to the beginning. They must evolve with user interaction and interpretation as the implications come into view.
- Planning and documenting is important, but following the plan documenting details is not as important as satisfying the customer with a solution that works correctly.
- The systems engineering and management processes emerge to fit the circumstances and control metrics are empirically determined. The methodology does not specify this ahead of time. (Barber et al. 2011, 2)

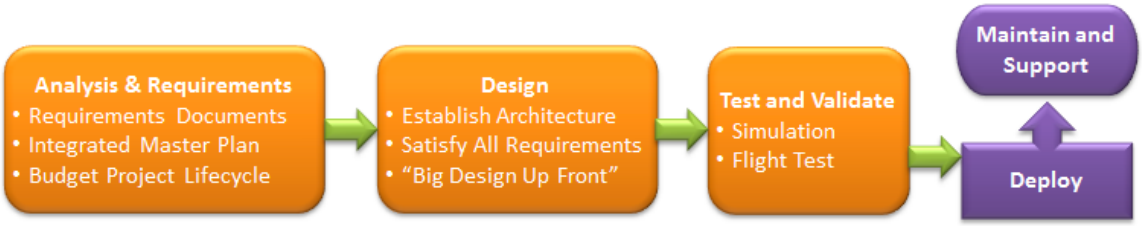

Figure 7. PD-PLDC "Waterfall" Methodology. Source: Barber, Montague and Barello (2011).

Barber et al. advocated that an Agile methodology was most effective when the following conditions exist:

- Requirements are unstable or evolving.
- All stakeholders (customers, managers, developers, testers) are in a position to collaborate as requirements evolve.
- Technical innovation is essential to achieve required capability. For some programs, innovation is not just "bonus" from clever engineers, but an outright necessity for the success of the effort. (Barber et al. 2011, 2)

Usage of Agile methodology, shown in Figure 8, has proven successful in the production of some PADSs, especially when the level of engineering effort and complexity require it. Barber et al. stated that adjusting requirements, iterated delivery and face-to-face interaction was a superior method for system engineering, and the idea is sound. The Agile methodology can be applicable to projects of a certain size and technical complexity, though it offers no increased guarantee of delivering a product on time and on budget when compared to the typical DOD Acquisition Framework.

Lastly, Barber et al. discussed the architecture decisions made through the development of their JPADS design. They stated:

> Good architecture also supports cost-effective development, not just the resulting design. Top level architecture decisions evident in the resulting JPADS design include:
>
> - common User Interface across platforms (LCD Screen, Mission Planning, Rigging etc.)
> - common Avionics and flight software across all platforms
> - open Source Operating System
> - flight software extensible to new canopy designs and control techniques
> - suspended-type AGU
> - tool-less connections between parachute and AGU
> - easy software upgrade
> - easy access to flight log data
> - common canopy structural and planform features to maximize commonality and simplicity of packing and rigging (Barber et al. 2011, 9)

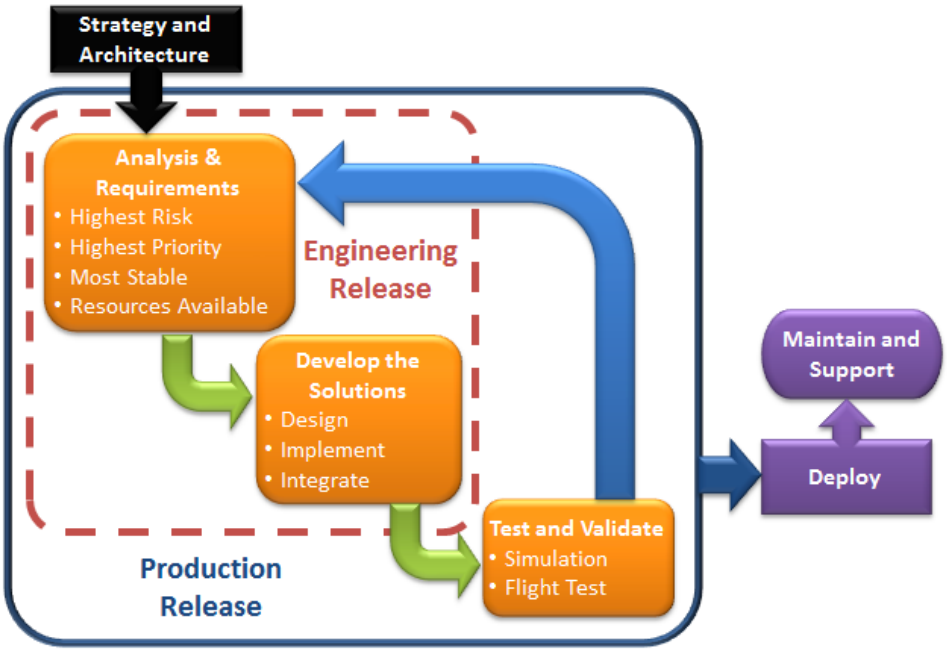

Figure 8. Airborne Systems Agile Methodology for U.S. DOD Programs. Source: Barber, Montague and Barello (2011).

I. SUMMARY

This chapter summarized some of the recent research relevant to the development of PADSs, including weight class definitions and the history of the JPADS program. This chapter also described the potential applicability of PADSs beyond logistical resupply to additional mission areas. The aerodynamic fundamentals of ram air parachutes were briefly discussed, as well as an introduction to the terminology used in the development and testing of PADSs. Subsequently, previous NPS research in the development of the Blizzard AADS, as well as methods for updating and enhancing PADS navigational accuracy were presented. Standard MOPs and MOEs used for the development of PADSs were described, as well as a summary on the utility of Agile methodology in systems engineering. The author's application of traditional and Agile systems engineering methodologies to design a low-cost micro-light weight PADS are detailed in Chapter III.

III. SYSTEMS ENGINEERING METHODOLOGY

A. CONCEPTUAL AND PRELIMINARY DESIGN OVERVIEW

Conceptual and preliminary design phases of a systems engineered project have several activities and interactions that must be accomplished to ensure the design is related to an actual stakeholder need responding to a perceived or actual problem. Blanchard and Fabrycky highlight several of these steps shown in Figure 9. This chapter will focus on several activities within these phases that assisted in the design and development of several prototype micro-light weight class PADSs, as well as some of the architecture decisions made through the design phase of an update to the NPS Snowflake. While preliminary design of a micro-light weight class PADS was geared toward operational employment, it is essential to note that the author did need to make significant deviations from an operational employment scenario to support adequate field testing and experimentation. In a sense, the author became the primary stakeholder of the preliminary design, as it was designed to support a more successive development that would more closely match an operational stakeholder need.

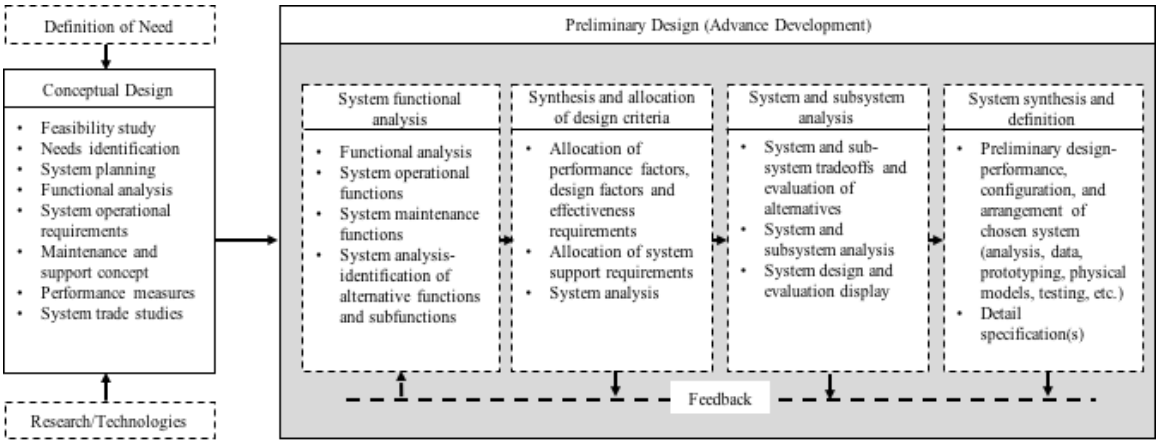

Figure 9. Technological Activities and Interactions within the Design Phases. Adapted from Blanchard and Fabrycky (2011).

B. PROBLEM DEFINITION AND NEED IDENTIFICATION

Many of the approaches to developing and constructing PADSs of all classes are derived from the three core COIs identified earlier. Continued exploration and research into other potential mission areas for micro-light weight class PADSs warrants a revalidation of the basic problem definition and identification of a hypothetical stakeholder's needs. The core problem surrounding any type of precision aerial delivery is that there is a person, unit or organization that needs (or wants) something that it does not have. Aerial delivery is more suited for longer ranges between the current location of the equipment and its intended location. Additionally, if time is a concern, the speed of aerial delivery over extended ranges is preferred over alternative means.

From a military perspective, the presence of hostile or adverse factors impeding delivery is a concern and can make aerial delivery a preferred option. In consideration of the hostile factors, the effective need is for delivery with a minimum of risk to the delivery method as well as to the intended recipient. For example, if preparation of a helicopter-landing zone presented an increased risk to isolated military forces, then the forces may well consider whether the logistical supply was necessary. The cost associated with larger classes of PADSs have been accompanied by the effective requirement that the unit being supplied collect and return the PADS for subsequent reuse.

In addition to the operational utility of employed PADSs, the micro-light weight class design engineered for this thesis also presented a secondary set of needs. It needed to preserve and retain experimental data, to survive repeated flight experiments, to be compatible with available launch platforms and parafoils, and finally, to support the development of an ADS that could match or exceed previous designs.

In summary, the combined problem that users, developers and researchers have is that there is the need for a proven, reliable method to distribute rapidly, responsively and efficiently physical items from one location to another at potentially medium to long ranges while incurring no additional threat from hostile forces.

C. STAKEHOLDER ANALYSIS

A more thorough investigation of the applicable stakeholders, their effective needs and concerns is shown in Table 2. As the author's updated version of the Snowflake was not designed for a particular customer, the interests of the stakeholders represented are generalizations only, based on information collected from various unclassified sources, primarily the ONR AACUS CONOPS (ONR 2012, 3–4). Various humanitarian aid and non-governmental organizations (NGOs) are also potential customers interested in the development of micro-light PADSs. Additionally, the author's needs are included with the NPS needs, as it is significant to highlight that successful research and development are still required to develop solutions targeting the original problem statement.

Table 2. Micro-Light PADS Stakeholder and Needs Analysis

Stakeholder	Type	Need	Want	Concern
ONR	Current	Research and technological development of solutions to long-term capability shortfalls	Technology that can provide benefit and utility for additional capability shortfalls	Solutions are too specific and fail to address the core problem statement
USMC	Current	Dispersal of time critical logistic support to dispersed units	Autonomous delivery and the ability to extract wounded military personnel	Likely operational environment includes hostile threats. PADSs must be supporting units, not units supporting PADSs.
NPS	Current	Suitable platform for research and development	Low-cost with minimal complexity and the ability to work with non-specialized equipment	Platform and results must be easily transferrable
NGO	Potential	Rapid dispersal of logistics to specific locations,	Long range, inexpensive and reliable	Must be more suitable in terms of cost or simplicity than existing alternatives
USN	Potential	Dispersal of logistics to mobile platform	Rapid, long range distribution at sea with minimal operational impact	Must be more suitable in terms of cost or simplicity than existing alternatives

D. DESIGN CRITERIA

In re-designing the Snowflake, the author considered the factors shown in Figure 10 contrasted with some of the design considerations required to field the operational system shown in Figure 11. The blue design considerations are common between the NPS Snowflake and an operationally fielded micro-light PADS. The considerations shown in green are unique to an operationally fielded system. Conceptual and preliminary system design considerations for a research-focused system in development differ from those of an operationally fielded system. More significantly, the prioritization of these design considerations, regardless of the system's objective, evolves during development.

Figure 10. System Design Considerations for Research Focused NPS Snowflake. Adapted from Blanchard and Fabrycky (2011).

Figure 11. System Design Considerations for Operationally Fielded Micro-Light PADSs. Adapted from Blanchard and Fabrycky (2011).

Table 3 presents the shifting emphasis between a research-focused developmental design and the design considerations associated with an evolved system. This fluidity of design has potential peril in that the developmental design can begin to migrate away from the original problem statement and effective stakeholder needs.

Table 3. Contrast of Design Consideration Emphasis During Preliminary Design for Research Focused NPS Snowflake and Operationally Fielded Micro-Light PADSs

Design Consideration	Research-Focused NPS Snowflake	Operationally Fielded Micro-Light PADSs
Flexibility	Support diverse research and testing objectives as they are developed	Support customer needs and wants as they evolve
Interoperability	Interoperable with available test platforms	Interoperable with all fielded systems
Safety	Controlled environment with trained users	Potentially hostile and adversarial environment with minimally trained users
Reliability/ Maintainability	Adequate to support multiple scientific experiments. Failures are expected.	Customer expects high reliability. Impact of failure can be catastrophic.
Technical Feasibility	Must be accomplished by two-person team within 6–9 months	Greater opportunity for technical advancement and solutions
Consistency	Consistent data collection is paramount in development	Consistent performance is paramount in operation
Supportability	Limited support during testing at Camp Roberts	Potential requirement to be supported in austere locations
Human Factors	Only 1–2 specialized operators	Must be able to work with 5–95% percentile operator
Maintainability	Must be able to conduct multiple experiments in short period of time	Potential to be single use only
Affordability/ Profitability	Research budget with no specialized equipment	Potential economy of scale, but profitability is significantly weighted priority
Functionality	Flexible for various experiments	Flexible for various missions
Producibility	Short timeline with minimal specialized equipment	Production costs are concern, but unknown in development
Product Quality	Not a concern	Customer demands high and consistent product quality
Recyclability/ Disposability	Not a concern	Potential to be a significant concern as the units may not be recovered
Environmental Sustainability	Not a concern	Warrants significant attention based on customer needs
Social/Political Feasibility	Not a concern	Warrants significant attention based on customer needs

The author's initial design considerations matched those of the operationally fielded design but migrated as the objectives and effective stakeholder needs evolved. Effectively, the author became the primary stakeholder, with successful thesis completion emerging as the primary problem statement. To support this objective, the emphasis on data collection and failure mode correction emerged as paramount.

E. ARCHITECTURE DECISIONS

As the emphasis for design considerations evolved during the conceptual and preliminary phases, the architecture was designed to incorporate a high degree of flexibility, modularity, maintainability and consistency. Since flight experimentation for the NPS Snowflake needed to be completed in one-to-two day periods of data collection and initial designs exhibited low component experimental survivability, the author emphasized modularity within the design. As guidance computers, control actuators, parachutes and telemetry components frequently did not survive even the reduced impact forces at landing, the design prioritized the ability to replace damaged components with a minimal amount of down time. Additionally, there were several ram-air parachute designs that would be tested, so the design incorporated the modular concept to facilitate parachutes that could readily be transferred and repacked in the field.

In addition to the high degree of component modularity, initial designs required an architecture that could support flexibility. Prototype systems are likely to change significantly and eventually converge on a preferred design. Working with a limited timeline and budget, the author desired a flexible architecture that could support multiple design changes and adaptations.

F. OPERATIONAL CONCEPT

The operational concept for employment of precision airdrop combat delivery missions is shown in the Department of Defense Architecture Framework (DODAF) Operational View (OV) shown in Figure 12. This does not represent all of the potential uses for PADSs, as it is specific for a combat logistical delivery over land. However, the core concept is that there is a demand to deliver something to a remote location, within a certain threshold for accuracy. The exact composition of the payload and the intended coordinates are transmitted to a command and control node along with an aggregated weather and winds estimate to compute an optimized CARP. In general, PADSs can vary from supporting long-term strategic objectives to supporting small-scale urgent resupply to troops in contact. Additionally, though the OV-1 depicts a large fixed-wing cargo

aircraft, the operational concept is equally valid for all types of aerial delivery platforms, including UASs.

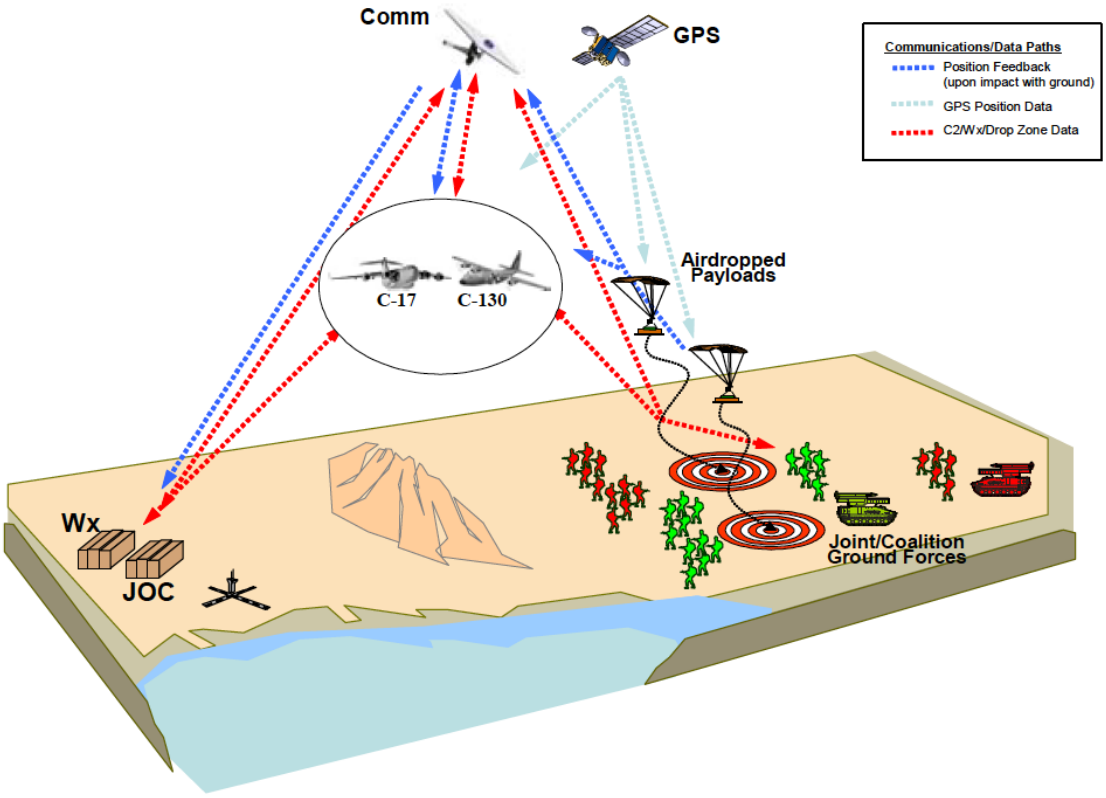

Figure 12. Precision Airdrop Combat Delivery Missions (OV-1). Source: Benney et al. (2005b).

G. FUNCTIONAL ANALYSIS

Blanchard and Fabrycky state that functional analysis in the early conceptual and preliminary design phases allows the engineer to generate detailed design criteria, as well as to identify the resources required. (2011, 86) With consideration to the complexity of a prototype PADS, the author derived and continually adjusted a functional hierarchy and the associated descriptions of the functions.

1. Functional Hierarchy

A functional analysis was performed by the author to decompose the mission of preforming the aerial resupply mission. The author's intent was to decompose the core functions required to complete the mission. Along with the core mission functional hierarchy shown in Figure 13, the secondary mission of performing design experimentation is evident. Initial PADS prototypes were constructed to perform the core mission, but significant adjustments were required to support design development and testing. The additional functions, shown in green in Figure 13, were unique functions incorporated into the Snowflake ADS simply to support development, but the author did feel it was significant to highlight the degree to which initial designs effectively had missions of their own. These functions were derived from design requirements that were generated through discovery during testing.

Application of the systems engineering methodology through functional analysis proved extremely useful. Rather than focus on component specific solutions to problems encountered during development, the author frequently returned to the first and second level functional decomposition to determine the root function being performed. This functional analysis was effective in focusing the design effort toward the *what* needed to be accomplished, versus the *how* it was to be achieved (Blanchard and Fabrycky 2011, 86).

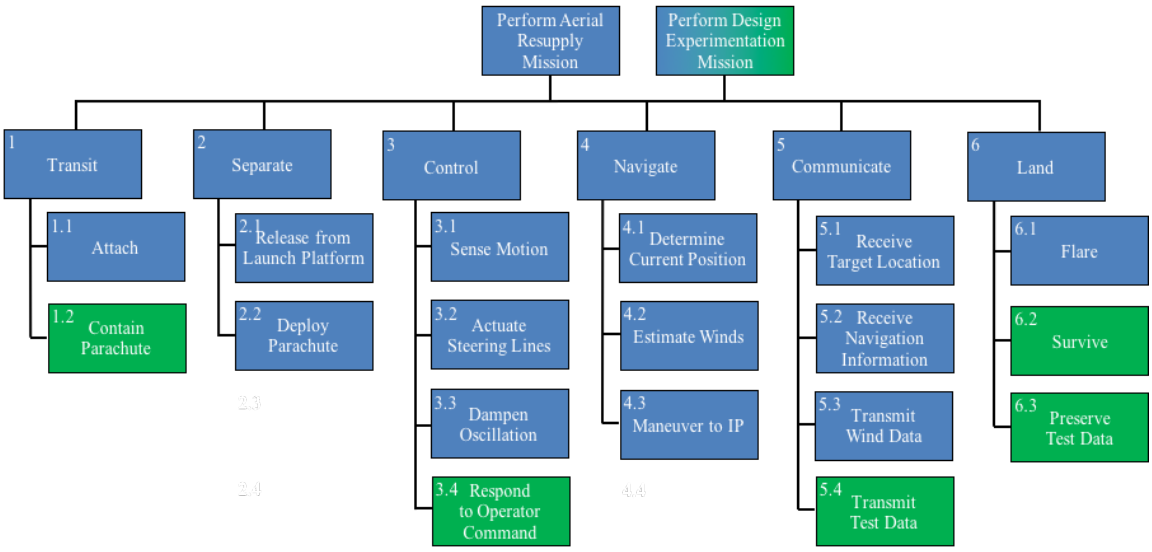

Figure 13. Functional Hierarchy of Two PADS Missions

2. Description of Functions

Each of the functions that the PADS was designed to perform is described in Table 4. Only the first and second level functions are shown, and though several state functions such as "to be affordable," "to be flexible" or "to be supportable" were significant concerns during design, they are not characterized as functions that the PADS would perform.

Table 4. Description of Functions

Number	Function	Description
1	Transit	Transit from launch location to CARP
1.1	Attach	Secure to launch platform (significant for externally mounted PADSs on UAVs)
1.2	Contain Parachute	Contain parachute from launch to CARP (significant for externally mounted PADSs)
2	Separate	Safe separation of PADS from launch platform which does not damage or place either component at risk
2.1	Release from Launch Platform	Release from launch platform with required arming and release functions performed
2.2	Deploy Parachute	Actuate release mechanism allowing parachute bag to open and parachute to deploy
3	Control	Execute control of the PADS through steering line retraction
3.1	Sense Motion	Measure and record current PADS attitude and acceleration
3.2	Actuate Steering Lines	Release and retract opposing steering lines during flight
3.3	Dampen Oscillation	Control and reduce PADS roll, pitch, yaw oscillations
3.4	Respond to Operator Command	Respond to operator input during PADS flight by non-specified means
4	Navigate	Translate from PADS present position to desired IP
4.1	Determine Current Position	Measure PADS current location and altitude
4.2	Estimate Winds	Measure/calculate winds during descent profile
4.3	Maneuver to IP	Based on present positon and predicted wind, adjust profile to desired IP
5	Communicate	Communicate with operator
5.1	Receive Target Location	Accept input of desired target location
5.2	Receive Navigation Information	Accept input of present position and altitude
5.3	Transmit Wind Measurements	Transmit calculated wind estimation for subsequent PADSs
5.4	Transmit Test Data	Transmit compiled status and collected data for experimental analysis
6	Land	Impact surface
6.1	Flare	Maneuver control surfaces to reduce vertical speed on landing
6.2	Survive	Withstand surface impact for subsequent use/experimentation
6.3	Preserve Test Data	Preserve all flight test data for continues developmental testing

H. SUMMARY

This chapter provided a summary of the technical activities included in the conceptual and preliminary design phases. It also defined the core problem that PADSs are designed to resolve and subsequently identified the basic functions that the system needs to execute in both an operational and experimental settings. The needs, wants and concerns of several stakeholders were detailed, as well as the design criteria that drove conceptual design. Points of contrast between operational and experimental system design criteria were highlighted. The chapter included several architecture decisions and described the influence of shifting design considerations on the architectural development. The operational concept for PADS employment was discussed and a functional analysis was specified. The application of the described systems engineering methodology to the development of the prototype Snowflake ADS is detailed in the following chapter.

THIS PAGE INTENTIONALLY LEFT BLANK

IV. BLIZZARD SYSTEM COMPONENTS AND SNOWFLAKE ADS DESIGN

In order to conduct initial and preliminary design experimentation, the updated Blizzard system consisted of the following four components: an Arcturus UAV, a modular AGU, a series of ram-air parachutes and the release/separation interface between the launch platform and the AGU. All of the components were required to perform the functions necessary to conduct a PADS experiment, and each is described in detail in this chapter. As initial and preliminary design is a highly iterative process, several of the early and intermediate designs have been omitted, except as noted. The Snowflake ADS design incorporated a high degree of modularity and flexibility in order to facilitate controlled changes to each of the components to correct expected and unexpected failure modes. Additionally, a comparison of the flight control dynamics between a conventional fixed-wing platform and the flight control dynamics of a ram-air parachute are described because the limitations presented proved significant in the construction and implementation of a functional ADS.

A. ARCTURUS T-20 AND JUMP 20

The Snowflake ADS was designed to maximize compatibility with any available UAV launch platform that could both support testing and potentially serve as a component in an operational Blizzard AADS. Fortunately, two versions of UAVs were available and used to support flight-testing at McMillan Airfield, Camp Roberts, CA: the fixed-wing Arcturus T-20 and a more advanced VTOL version called the JUMP 20. Specifications for each of the UAVs are shown in Table 5. During testing, the author would generally receive two-to-three-week's notice of which type of UAV would be available, requiring the Snowflake ADS to be designed to support compatibility with diverse launch platforms with minimal modification.

Table 5. Comparison of Arcturus UAV Specifications Adapted from Arcturus UAV (2015a and 2015b).

Specification	T-20	JUMP 20
Type	Conventional using pneumatic catapult launcher	Vertical Takeoff and Landing (VTOL)
Airframe	Airframe monocoque composite	Airframe monocoque composite
Wing Span	17’ 6”	18’ 6”
Length	9’ 5”	9’ 5”
Engine	190cc 4 Stroke	190cc 4 Stroke
Fuel	MOGAS	MOGAS
Typical MTOW	185 pounds	210 pounds
Typical Max Speed	75 kts	72 kts
Endurance	10-20 hours (payload dependent)	9-16 hours (payload dependent)
Payload Capacity	75 pounds	60 pounds
Main Payload Bay	4,100 cubic inches	4,100 cubic inches
Rated Ceiling	15000’ (proven to 25000’) MSL	15000’ MSL
Guidance	Full autonomous operation, launch to land	Full autonomous operation, launch to land
Characteristics	Flight and recovery under austere conditions	Flight and recovery under austere conditions

1. T-20

The T-20 is a fixed-wing fully autonomous UAV which had previously conducted research support with the Blizzard AADS and is shown in Figure 14. The T-20 offers slightly greater range, altitude, endurance and payload capacity when compared to the JUMP 20. However, it requires a relatively large pneumatic catapult for launch as well as a prepared surface for landing. The T-20 supported Snowflake payload deployment from either wing as well as conducting multiple deployments during the same flight. The T-20 could reach launch altitude within roughly five minutes and required only minutes to conduct post-flight maintenance inspections and subsequent pre-flight and startup procedures. As such, the T-20 could support close to two experimental flights per hour.

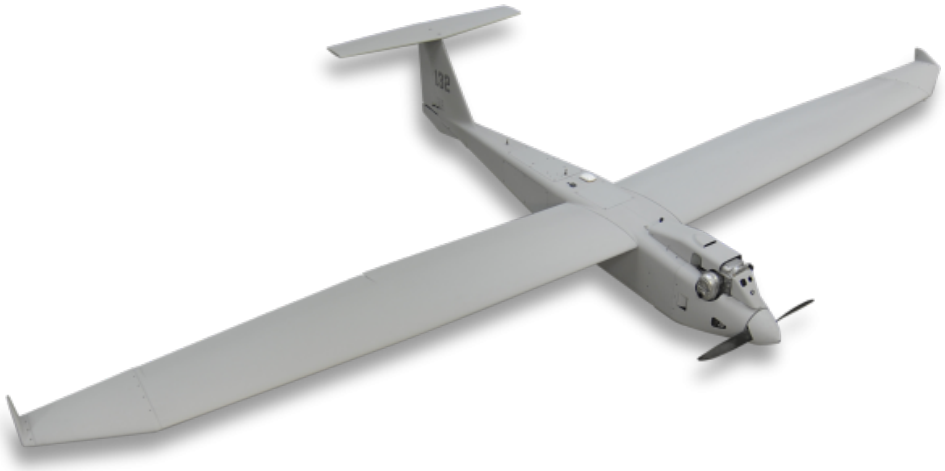

Figure 14. Arcturus Fixed-Wing Version (T-20). Source: Arcturus UAV (2015a).

2. JUMP 20

The JUMP 20, shown in Figure 15, is a more advanced version of the T-20 which is designed to conduct VTOL operations. The VTOL capability offers a significant enhancement for shipboard operations where launch and land spaces are limited. The JUMP 20 does have a slightly reduced range and shorter endurance when compared to a conventional fixed-wing UAV. As it did not require a pneumatic catapult, the JUMP 20 had centerline fuselage mounting stations in addition to the under wing stations. Unfortunately, its payload capacity is slightly smaller than the T-20, which would decrease its operational utility slightly. Additionally, when conducting flight experimentation, the JUMP 20 required significantly longer to reach an operational altitude and the time between launches was roughly twice that of the T-20. The post-flight electric charging requirement reduced the availability of the JUMP 20 by roughly 50% as compared to the T-20.

Figure 15. Arcturus VTOL Version (JUMP 20). Source: Arcturus UAV (2015b).

3. Integration

Despite efforts to construct a Snowflake ADS that required minimum integration with the launch platform, the author remained subject to some distinctive differences in operation between a catapult-launched fixed-wing UAV and a VTOL UAV. Launches from a T-20 subjected the Snowflake to an acceleration of approximately 5 Gs. As such, the internal components needed to be tightly secured and the external parachute container needed to be sufficiently robust to prevent parachute release shortly following launch. In contrast, the VTOL JUMP 20 had a very smooth and controlled launch acceleration of approximately 1.2 Gs, which did not stress the parachute container on takeoff.

Though the JUMP 20 did not subject the Snowflake to the stress of a catapult launch, there was a much smaller threshold for harmful interference between the UAV and the Snowflake ADS. During the takeoff, landing and transition to and from forward flight, the vortices generated by the four rotors created highly turbulent airflow around the wing and the Snowflake. As such, the mounting hardware, static lines and parachute

deployment lanyards all had to be short enough to prevent harmful interference with the rotors. The relatively tight tolerances for mounting hardware presented a small, but manageable integration challenge between the two systems, but these were necessary precautions to prevent an increased risk of a catastrophic failure.

B. AUTOMATED GUIDANCE UNIT

The Snowflake ADS was composed of three elements: an AGU, a parachute, and the release/parachute deployment mechanism. Various iterations of the AGU were constructed during development, with the preponderance of effort focused on two different flight controllers and a power distribution design that would facilitate development, testing and repeated experimentation. The following section details the specifics and implementation of each type of flight controller, as well as the final design for a power distribution bus.

1. Prototype with Pixhawk Flight Controller

The Pixhawk flight controller from 3D Robotics, as shown in Figure 16, was initially chosen as a low-cost automated guidance unit. The Pixhawk is a commercially available, customizable, navigation and control platform used widely through the hobby and commercial UAV industry. The Pixhawk offers a three-axis gyroscope, a three-axis accelerometer/magnetometer, an onboard barometer for detecting altitude changes as well as integration for an external GPS receiver. The author also utilized the Pixhawk's radio control integration to assist in developmental testing and to conduct controlled flight experiments.

Figure 16. Pixhawk Flight Computer and Installation in Prototype Snowflake ADS

In addition to the previously described features, the Pixhawk was designed to be configurable for a variety of UAV platforms, to include multiple types of copters, ranging from one to eight blades, land-based roving vehicles and conventional fixed-wing aircraft. Working in conjunction with Lieutenant Commander Matthew O'Brian, the author determined that the Pixhawk would be able to provide satisfactory guidance and control for the Snowflake ADS at a sufficiently low-cost that operational employment in a one-time-use scenario would prove feasible.

The prototype AGU also included two Turnigy TGY-6114MD digital sail winch servos secured to a custom-built mounting board made of G-10 glass epoxy composite laminate. Early designs utilized commercially available polycarbonate sheets, but the polycarbonate was not sufficiently strong to support all components under stress or to absorb the landing shock associated with an ADS touchdown. The Pixhawk and the servos were powered using a 2200mAh 7.4V 2-cell lithium polymer battery, which would provide adequate power for a roughly 20-minute flight. The author opted not to use a larger battery, theorizing that weight conservation in design would provide additional flexibility throughout development and ballast could be added if required. Finally, the

design included a HobbyKing HKU5 5V/5A battery eliminator circuit (BEC) to isolate servo power from the Pixhawk guidance unit.

Externally, the author intended to inherit the parachute bag from the previous Snowflake ADS, but initial flight-testing proved nearly catastrophic as detailed in Chapter V. Following the initial flight tests, the parachute bag was redesigned by a small team consisting of the author and Major Alan Stephens as an element of the SE3201/SE3202/SE3203 design project course. In addition to correcting a potentially hazardous failure mode, the updated design was created to support the flexibility design consideration. The updated parachute bags, shown in Figure 17, would accommodate diverse parachute sizes and shapes as well as multiple release methods. As a final design had not been determined yet, the parachute bags were primarily designed to support repeated flight experimentation. The author planned to create a more fit-for-purpose design as development converged on a preferred parachute size, type and release method. Unfortunately, the design did not converge on a single parachute design and release sequence until after the author's final flight-testing opportunity at McMillan Airfield in February 2016.

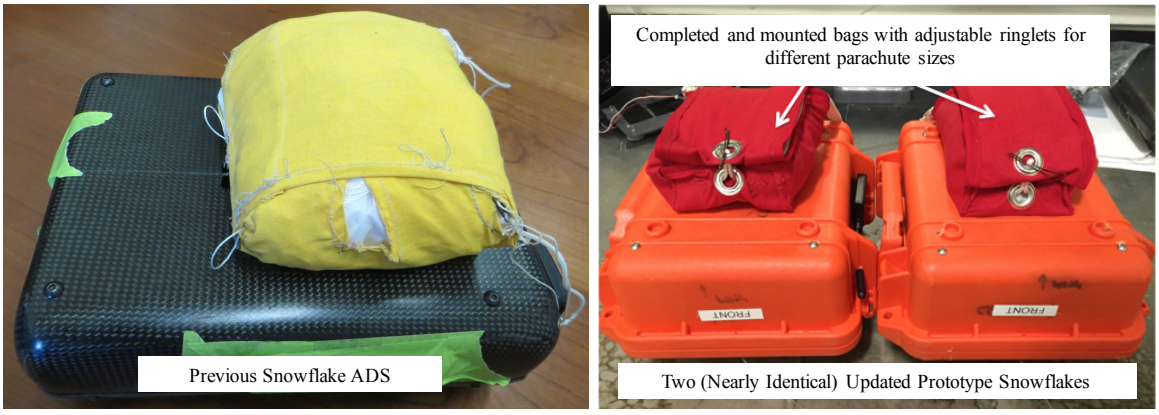

Figure 17. Snowflake ADS Parachute Bag

2. X-Monkey Flight Controller

Following some of the experiments detailed in Chapter V, the design of the AGU evolved to incorporate a new flight controller more suitable for guidance, control and

experimentation. The X-Monkey from Ryan Mechatronics is a similar autopilot as the previously described Pixhawk, with three-axis gyroscopes, three-axis accelerometers and magnetometers and an integrated GPS. The Pixhawk and X-Monkey are similar in terms of the function of the internal components, and the cost is roughly comparable. In selecting the Pixhawk, the author hoped to incorporate COTS technology with a minimum amount of modification to deliver the functions required of an AGU in a PADS. Unfortunately, the author struggled with the requirement to modify the Pixhawk with little to no technical support available. As such, the author converted to a design utilizing the X-Monkey. The X-Monkey offered less performance out of the box, but offered a much more open software development platform suitable for modification to autonomous parachute control. It also had a more proven history of success in supporting scientific experimentation. Most importantly, the manufacturer was extremely responsive to technical support requests and provided significant assistance in the adaptation of control and guidance algorithms.

In addition to the X-Monkey autopilot, the final prototype incorporated a Digi Zigbee 802.15.4 Radio module, which could be paired with the X-Monkey graphical user interface (GUI) for command and data transmission. Lastly, the final prototype was updated to include a 20-amp BEC/voltage regulator from Castle Creations. The internal components of the final Snowflake prototype, including the installed X-Monkey, are shown in Figure 18.

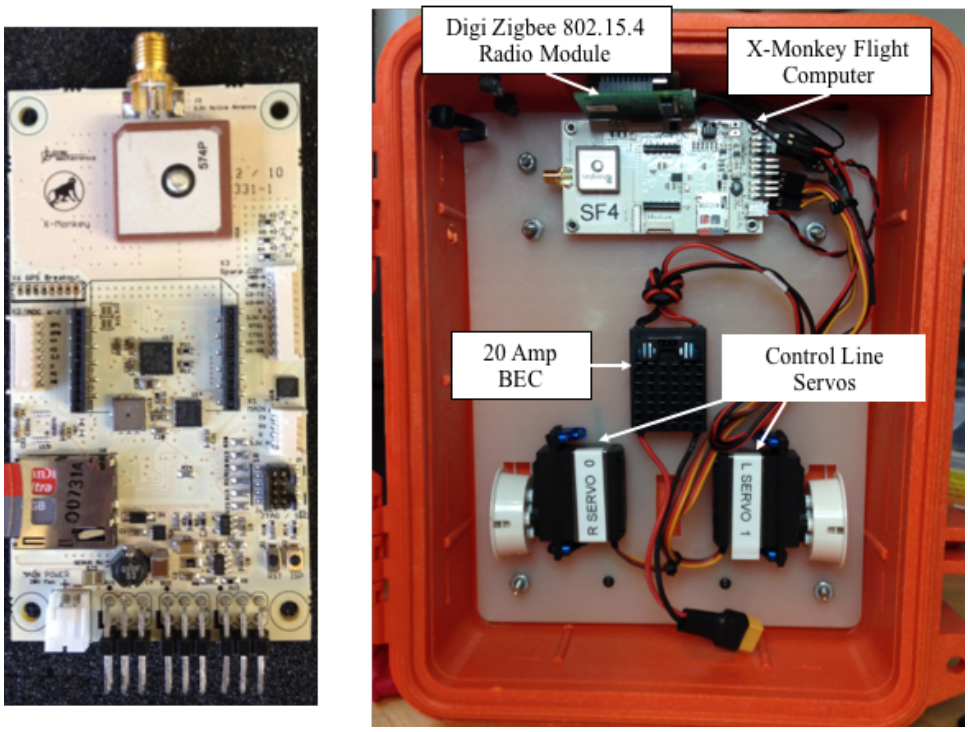

Figure 18. X-Monkey Flight Computer and Installation in Final Prototype Snowflake ADS

3. Power Supply and Distribution

The power supply and distribution sub-system for the Snowflake AGU consisted of relatively simple COTS components, but required some adjustment to eliminate the need for additional batteries isolating the autopilot. Since modularity and maintainability were principal design considerations, the author created and maintained a design that could provide the necessary power to each component, offer limited electrical isolation of the more sensitive components and still be simple enough that the wiring harnesses could be exchanged in the field with minimal down time. An operationally suitable Snowflake AGU would likely have a bit more fit-for-purpose design elements, but the schematic shown in Figure 19 supported Snowflake flight control as well as data collection.

As a Snowflake ADS flight experiment was roughly 20 minutes from power-up to landing, the relatively small 7.4-volt battery provided sufficient power to the control line servos, but a 20-amp capacity BEC was required to prevent the output from dropping below the five volts necessary to power the X-Monkey and to continue data recording.

Initial designs with a smaller capacity BEC occasionally caused the input power to the X-Monkey to drop below five volts and subsequently would trigger a reset. This reset would cause the X-Monkey to stop recording flight data for approximately five seconds and would reset the servo output commands to a neutral condition. The transient current spikes were caused by rapid reversals to the control lines or stalled conditions during parachute opening malfunctions.

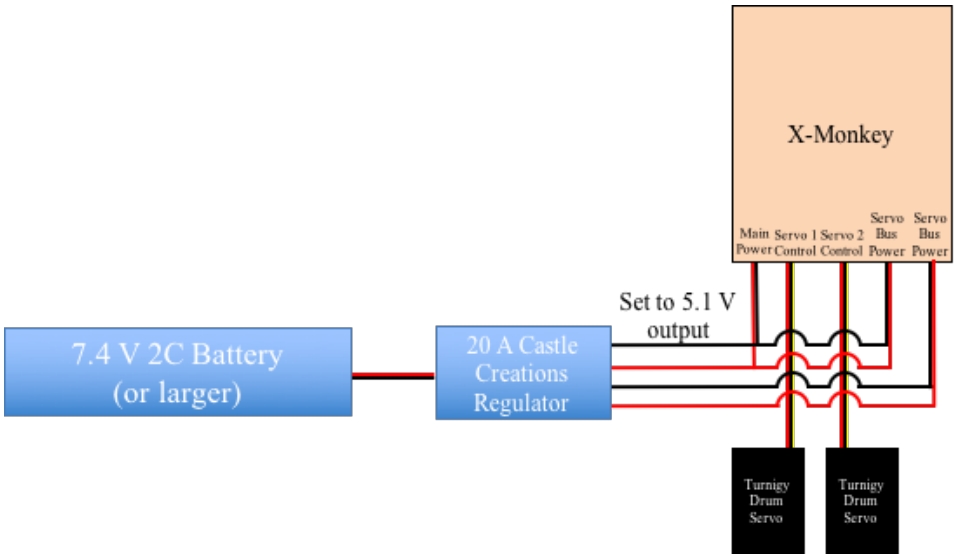

Figure 19. Electrical Power Distribution for Snowflake ADS

C. RAM-AIR PARACHUTE SPECIFICATIONS

Early design objectives were to incorporate a variety of available ram-air parachutes in order to evaluate which offered the best maneuverability and consistency. Unfortunately, several of the ram-air parachutes did not perform with sufficient reliability to asses and improve the design. As such, the implementation of each parachute is described below, with the final design converging on the rectangular ram-air parachute due to its relatively high build quality and consistent flight performance.

1. Elliptical Ram-Air Parachute

Initial designs for the updated Snowflake ADS were developed to utilize a commercially available elliptical ram-air parachute as shown in Figure 20. The elliptical

parachutes were a relatively low-cost design and offered the potential for enhanced maneuverability over the rectangular parachutes previously used in Snowflake ADS development. Preliminary experimentation indicated that parachute was approximately 10 ft^2, though exact measurements were not determined. The NPS ADSC Laboratory had a good supply of these elliptical parachutes, and they were initially thought to be suitable for repeated experimentation. Initial testing of the elliptical parachute conducted at NPS on May 1, 2015, as shown in Figure 20 demonstrated positive results, but it is significant to note that the tests were conducted with a nearly inflated parachute at release and the parachute bag had not been implemented yet.

Figure 20. Elliptical Ram-Air Parachute Preliminary Testing on May 1, 2015

2. Rectangular Ram-Air Parachutes

Rectangular ram-air parachutes were also utilized in the design and experimentation process and proved to be significantly more reliable during flight experimentation, though they offered slightly reduced maneuverability. Experiments were conducted utilizing rectangular ram-air parachutes of two different sizes, as the Snowflake ADS was designed to work with a series of weight payloads. The specifications for the rectangular ram-air parachutes used are show in Figures 21 and 22.

In addition to their increased reliability, the rectangular parachutes were easier to pack and their construction was of a much higher quality than the elliptical parachutes had. Numerous unsuccessful attempts were made during the research process to procure additional parachutes of differing sizes and shapes to support testing. Parachute manufacture can be extremely expensive and the normally high cost was compounded by the fact that there is presently very limited commercial utility for ram-air parachutes of this size.

Though these parachutes offered relatively consistent performance during testing, there is some stretching noted in the lengths of the control lines that can potentially affect controllability. Early testing of the prototype Snowflake ADS included some relatively high velocity openings that yielded a substantial opening shock, likely stretching the control and support lines beyond their elastic limits. Later prototypes had a reduced opening shock, but the author was not able to repair the support and control lines without risking damage to the only viable flight-testing platforms. Replacements were not available.

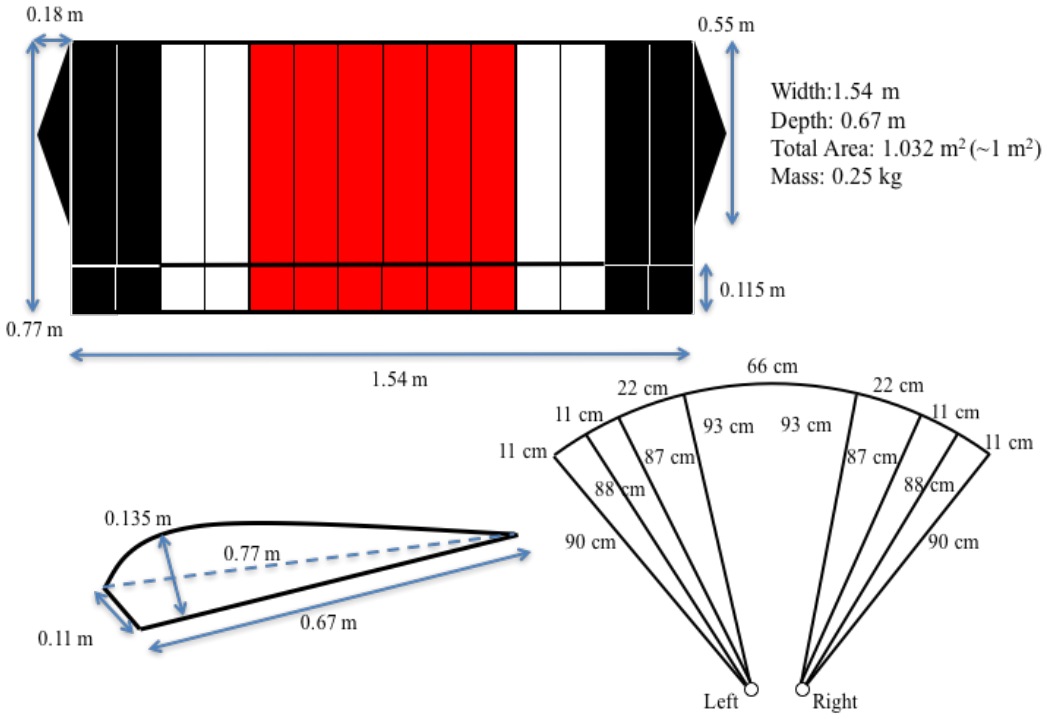

Figure 21. Overhead, Side and Control Line Specifications for 1 m^2 Rectangular Ram-Air Parachute

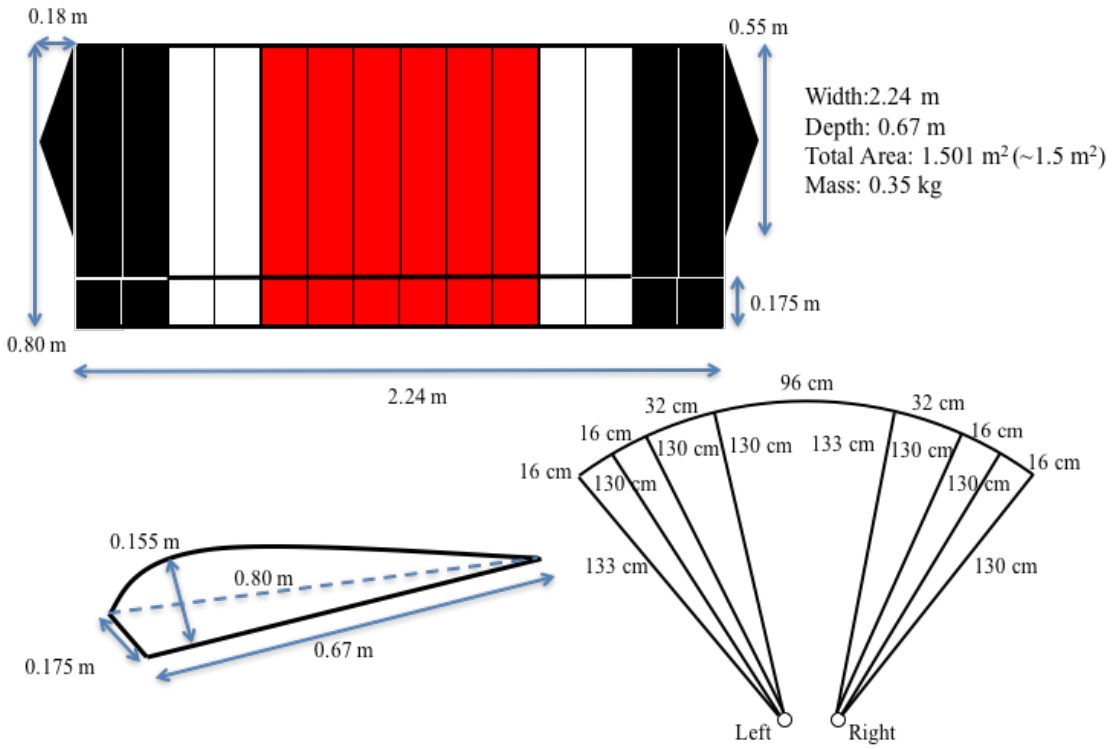

Figure 22. Overhead, Side and Control Line Specifications for 1.5 m^2 Rectangular Ram-Air Parachute

D. PARACHUTE DEPLOYMENT METHODS

When the Snowflake ADS was functionally decomposed in Chapter III, one of the first level function is "F2.0 To Separate." In conceptual design, the author assumed this would be a relatively simple function to complete and it could be accomplished with minimal complexity. Through the conceptual and preliminary design, three types of separation mechanisms were utilized, starting with a servo-actuated release, progressing to a static line release pin and finally to a double static line release.

1. Servo-Actuated Release

The initial prototype adapted the previously used design that incorporated a servo-release pin, that could be operator actuated by radio control or sensor actuated by the autopilot based on a combination of programmed conditions. This design sequence is shown graphically in Figure 23. A servo-actuated release was preferred initially because it would offer the capability for the Snowflake ADS to separate from the launch platform,

fall ballistically for a period of time and then open the parachute bag at an optimum altitude or location to minimize displacement error on landing. The author theorized that the Snowflake ADS could support release from medium altitude, reduce exposure time by falling ballistically and then deploy the parachute at the optimum moment. Additionally, this design required very limited integration with the launch platform. The Snowflake ADS could be mounted within seconds, and no additional attachments were required that would increase the complexity of the design. Though these were useful design features for an operationally suitable system, they were not required to support early testing.

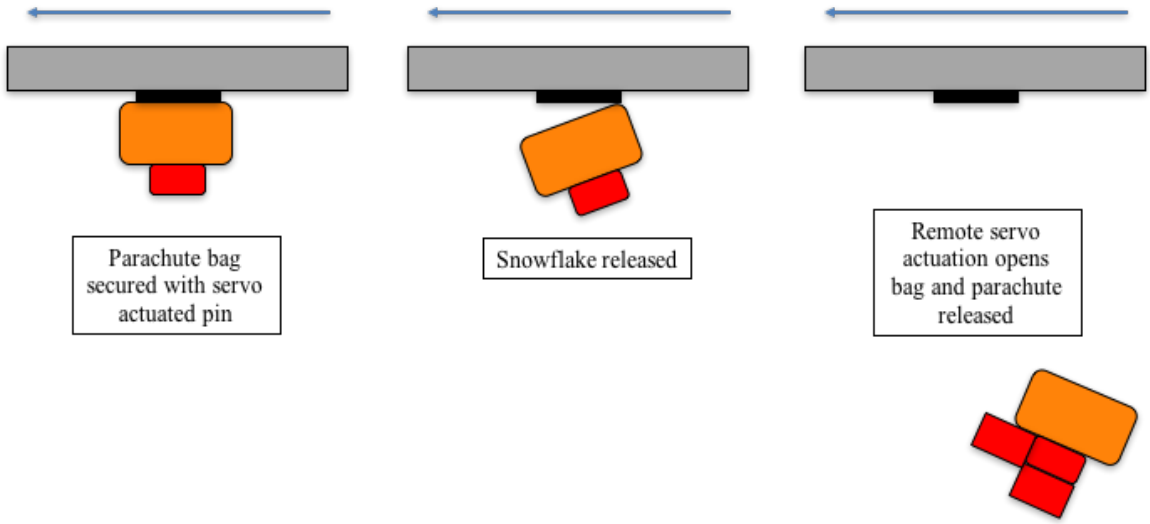

Figure 23. Servo-Actuated Release Sequence

Unfortunately, on the first two test flights, there was a pre-deployment of the parachute immediately after the JUMP 20 executed its transition from vertical to forward flight. Subsequent post-flight failure analysis determined there were two potential failures contributing to the pre-deployment: failure of the parachute bag to contain the parachute or premature actuation of the release pin due to an unknown condition. As the root cause could not be specifically determined and corrected, the design team implemented two changes to eliminate the potential of a reoccurrence: the parachute bag was fundamentally redesigned, and the servo-actuated release was removed until the possible transient behavior of the autopilot could be understood better.

2. Static Release Pin

Following the initial prototype, the static release pin sequence shown in Figure 24 was implemented. The parachute bag was kept closed by a cotter pin secured to the mounting block on the launch platform as shown in Figure 25. This design had a slightly higher integration requirement. The Snowflake had to be mounted under the wing with a static line attached for each flight. As the static line remained underneath the launch platform for the duration of the flight, the author had to consider any potentially harmful effects. Specifically, on the JUMP 20, the static line was approximately 12 inches from the spinning blade of the aft lift fan. There was no clearance issue during launch or forward flight; however, the design could not interfere with a high velocity propeller providing thrust during landing. With this consideration in mind, the static line had to be sufficiently long to release the cotter pin on the parachute bag, but only had about one inch before potentially impacting the lift fan. This requirement added roughly five minutes to the Snowflake ADS loading sequence as the static line had to be measured and confirmed separately for each Snowflake ADS.

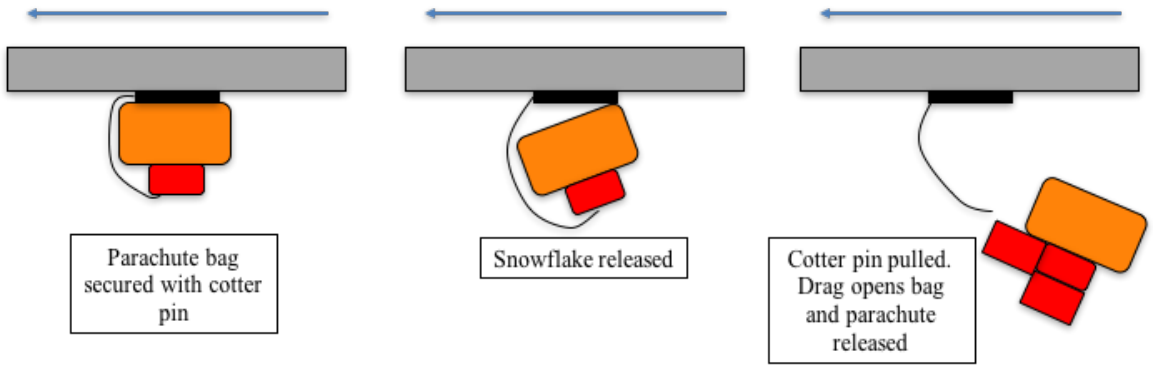

Figure 24. Static Release Pin Sequence

This design served to be robust and consistent, but following a series of failures in which the parachute did not deploy from the parachute bag, the design was adjusted to incorporate a second static line tether to assist in deploying the parachute immediately following release.

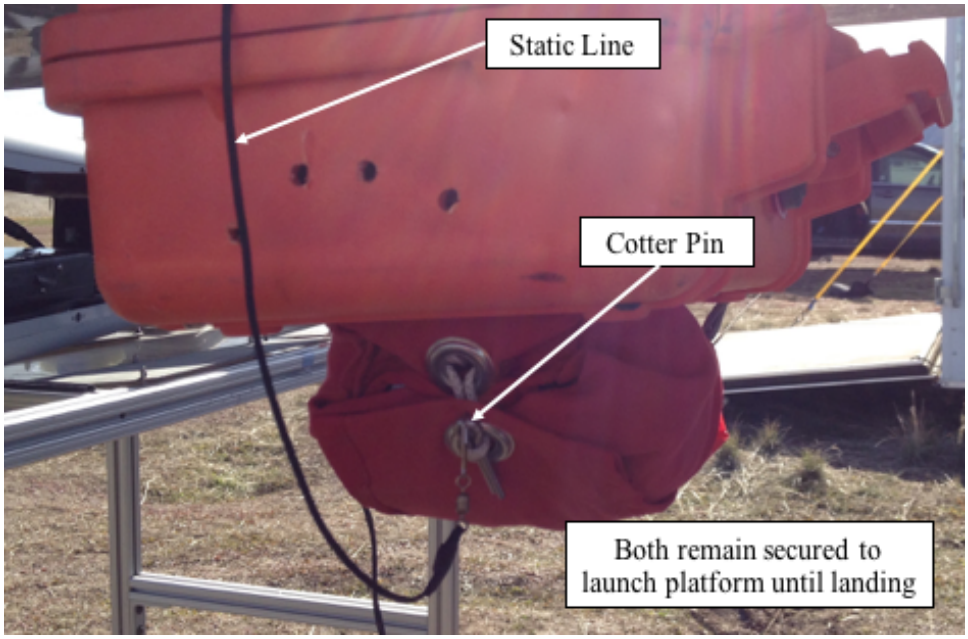

Figure 25. Installed Static Release Pin

3. Tethered Deployment

The double static line sequence, shown in Figures 26 and 27, was implemented on the final Snowflake ADS prototype to address repeated failures cleanly releasing and deploying a parachute. This design removed the capability of a servo-actuated release and could potentially limit the operational utility of the system. The author applied a systems engineering design methodology by characterizing the servo-actuated release as a desirable additional capability but not worth the associated complexity cost. In order to design a prototype that could support flight experimentation and data collection, the author adapted a double static line sequence that proved highly reliable and consistent for low altitude ADS flight profiles.

Given that the double static line method was still required to work on both types of UAVs, the requirement to minimize or eliminate destructive flight interference was present and included. Each parachute was fitted with an approximately six-foot lanyard to the middle of the upper surface of the ram-air parachute. The lanyard was connected to a 12-inch static line that remained secured to the mounting block on the launch platform. The lanyards were connected by two small rubber bands designed to break at

approximately six pounds of force, roughly equivalent to the weight of a Snowflake ADS. The six-foot lanyard was packed inside the parachute bag and would extend as the Snowflake was released and the parachute bag was opened. This second tether would provide a small but sufficient force to pull the parachute into the airstream and initiate inflation. As the inflation was initiated so quickly, the opening shock was minimized as well as the chaotic three-axis rotation that accompanied the release. The greatly reduced release dynamics contributed significantly to consistent parachute inflation suitable for control and precise navigation.

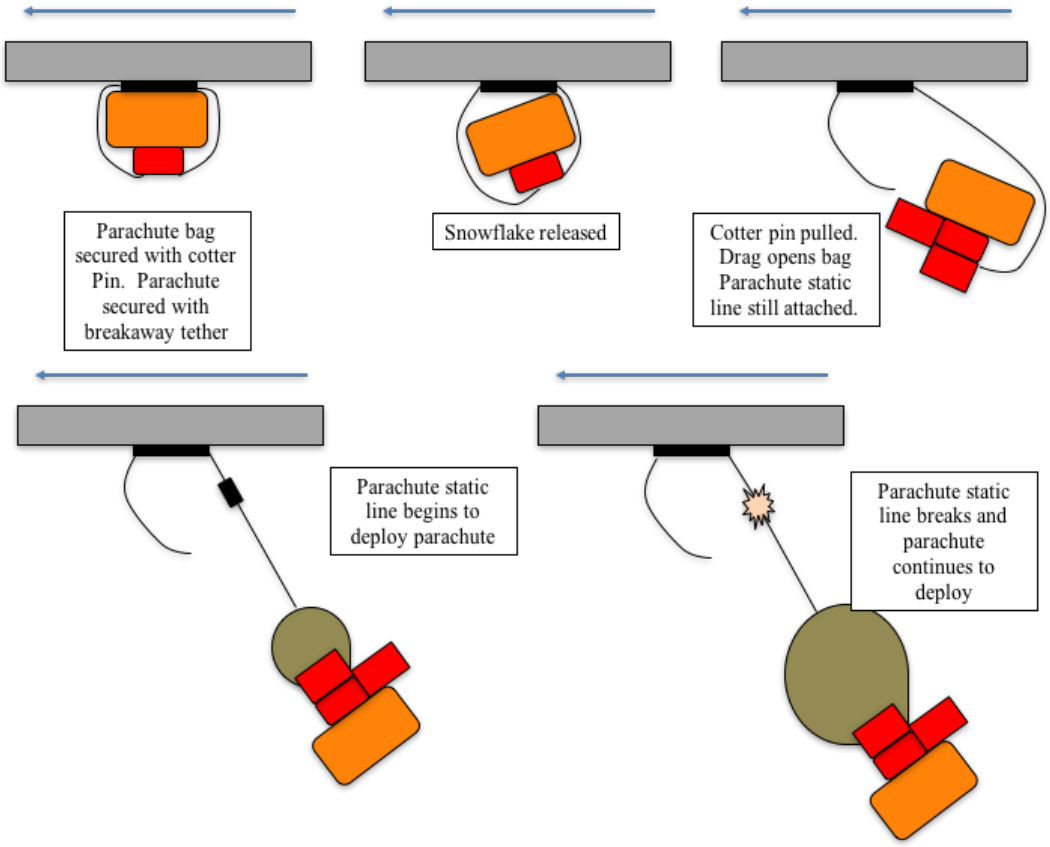

Figure 26. Double Static Line Deployment Sequence

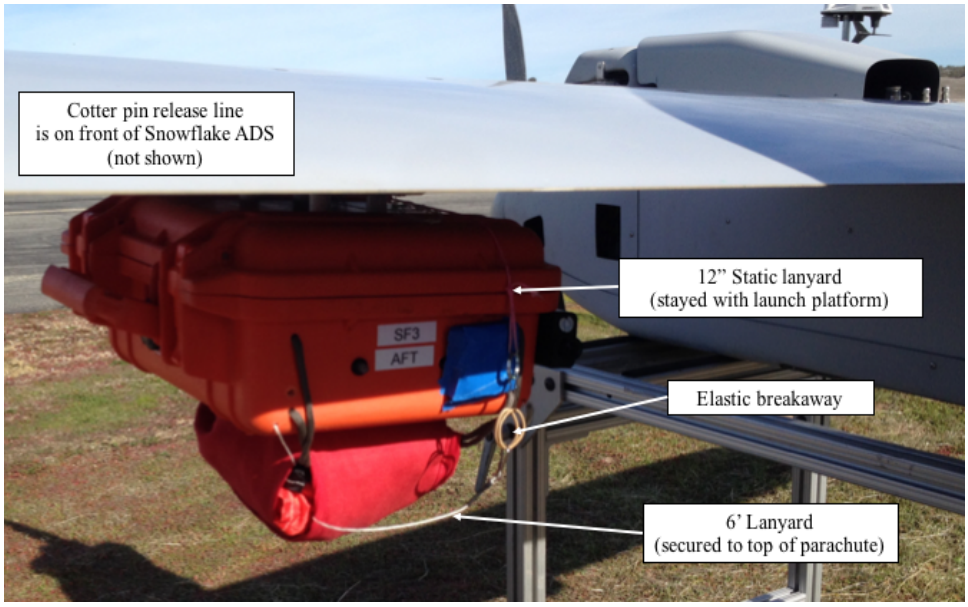

Figure 27. Installed Double Static Line

E. FLIGHT CONTROL DYNAMICS

The following section details some of the differences between the flight control dynamics of a fixed-wing aircraft and the flight control dynamics of a ram-air parachute. As most COTS flight controllers are designed to work with fixed or rotary-wing aircraft, it is essential to detail the subtle differences which preclude flight control of ram-air parachute with a fixed-wing dynamics without significant modification.

1. Fixed-Wing Aircraft

In addition to the results described in Chapter V, a comparison of the difference between the flight control dynamics of a fixed-wing aircraft and a ram-air parachute was essential in the selection of an appropriate flight controller. When considering that a principal design consideration was the use of COTS components because of their low initial cost, the author selected the Pixhawk autopilot as being one of the more developed units within the commercial autopilot industry. It offered a great deal of customizability for use in roving land vehicles, fixed-wing aircraft and multiple versions of copters. The author expected to adapt a fixed-wing profile for use in the Snowflake ADS as it was the most closely related.

The control inputs and associated platform responses of a fixed-wing aircraft are shown in Figure 28. Each control surface (ailerons, elevators or rudders) offers both a positive and negative control deflection to produce a platform response (roll, pitch or yaw). Though modern flight control systems often optimize and integrate these control surface deflections, the initial Snowflake design was to decouple them to develop a single input single output (SISO) model of the flight dynamics of each platform axis. The Pixhawk flight controller offered the ability to match the control surfaces shown, with some degree of customization to account for control surface travel limitations. Additionally, it did offer modes that utilized elevons to control concurrently both the roll and the pitch. Through experimentation, it proved extremely difficult to disable or minimize the aileron/elevon roll commands.

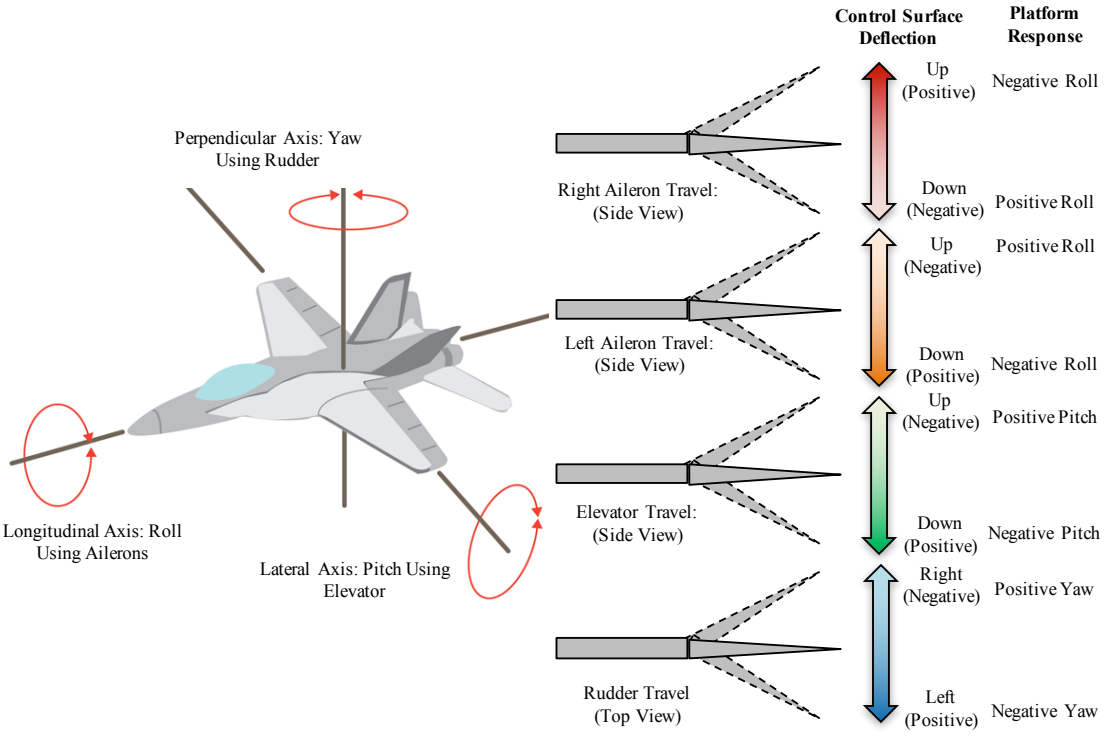

Figure 28. Description of Flight Control Inputs and Response of Fixed-Wing Aircraft

2. Ram-Air Parachute

In contrast to the fixed-wing flight dynamics, the flight control input to platform response of the ram-air parachute is shown in Figure 29. It is significant to highlight that

though controlling the pitch and roll of a guided ram-air parachute is still possible, the principal concern for initial design was maneuver about the perpendicular axis through yaw control in order to execute autonomous navigation. Unfortunately, the ram-air parachute does not offer a bi-directional platform response associated with bi-directional control surface deflection. Since the control lines can only be retracted, there is no way to cause a negative control surface deflection on the parachute. Consequently, the two control lines had to oppose each other, with each providing independent positive control deflection only.

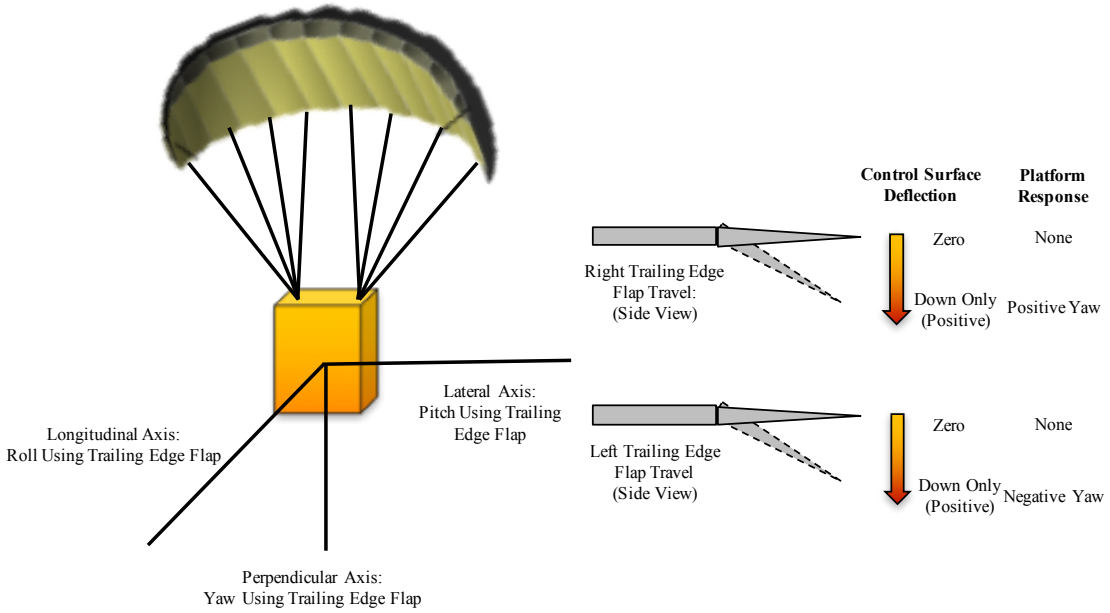

Figure 29. Description of Flight Control Inputs and Response of Ram-Air Parachute

The Snowflake ADS could also be expected to require pitch control in an effort to execute a terminal maneuver to minimize descent rate just prior to touchdown. This platform pitch could be accomplished with a concurrent positive control surface deflection. In contrast to the yaw control, which required opposing control surface deflections, a positive platform pitch can only be implemented by using paired positive control surface inputs.

3. Challenges during AGU Development

The differences between control of a fixed-wing platform and a ram-air parachute proved to be much more significant than anticipated. Moreover, the operating platform of the Pixhawk did not facilitate easy creation of a fully customized flight program. Unfortunately, there was minimal customer support provided to facilitate this customization. The Pixhawk did not offer the ability to offer opposing control line retractions to control yaw, the ability to decouple roll control inputs to produce a yaw response and the ability to provide synchronous dual control line pitch control.

As a result of these limitations, the author, in conjunction with Lieutenant Commander O'Brian, opted to switch to the X-Monkey flight controller due to its greater customizability and the availability of customer support.

F. SUMMARY

In this chapter, the conceptual and preliminary design of a Snowflake ADS and several additional components of the Blizzard AADS are described. The specifications for the two types of UAVs that were utilized in flight-testing are included. Subsequently, several iterations and a final prototype design are summarized, including the installation and usage of two types of autopilot computers. A description of the final design for power distribution is detailed, as early iterations contributed to unexpected failures in testing and experimentation. This chapter also includes a description of each type of ram air parachute that was tested, as well as the three types of UAV/Snowflake separation sequences. A comparison of the principles of flight control dynamics between fixed-wing platforms and a ram air parachute platform is incorporated, as it proved to be a significant challenge in the implementation of COTS technology. Comprehensive computer simulation and flight-test results of the various prototypes are detailed in Chapter V.

THIS PAGE INTENTIONALLY LEFT BLANK

V. COMPUTER SIMULATIONS AND FLIGHT-TEST RESULTS

Between April 6, 2015, and February 18, 2016, 65 live flight experiments were conducted at McMillan Airfield, Camp Roberts, CA. Additionally, there was a series of lab experiments performed in the ADSC laboratory at NPS before and following the February 2016 flight tests. This chapter details the results of those flight experiments, as well as the associated laboratory experiments, in preparation for planned flight-testing in May 2016 in support of Lieutenant Commander O'Brian's continuation of the research effort.

A. FAILURE MODES

This section includes separate failure analyses of the three types of parachute deployment methods, as well as compiled results on the success of both autopilot computers in performing the data recording function. Though a significant amount of effort was placed on prior lab testing, the uncertainty associated with live flight-testing continued to reveal unexpected weaknesses in the design.

1. Parachute Deployment Methods

The comprehensive results presented in Figure 30, show the various design iterations that the author incorporated during a nearly 10-month period. Following the nearly catastrophic results of April 6, 2015, the author converted from a servo-actuated release to a static release pin to simplify the design and prevent a potential reoccurrence of early canopy release. Once the risk of a catastrophic failure was reduced with the newly design parachute bag, the design emphasis shifted toward remedying a consistent problem of fouled or tangled parachute releases. All flight tests from April to June 2015 included the use of the previously discussed elliptical parachute design, which continued to deploy in an unpredictable fashion, frequently including full riser twists, line-overs and partial deployments. Initially, the author theorized that variability in the parachute packing technique was to blame for the inconsistent results but subsequently determined that the low manufacturing quality of the elliptical parachutes was a more likely cause. Additionally, the elliptical parachutes used cascade lines that were mounted laterally

across multiple cells rather than along the seam of a single rib. With only one clean and controllable parachute release in the first 10 flight tests, the author transitioned to the rectangular parachutes described earlier for the August 2015 flight tests.

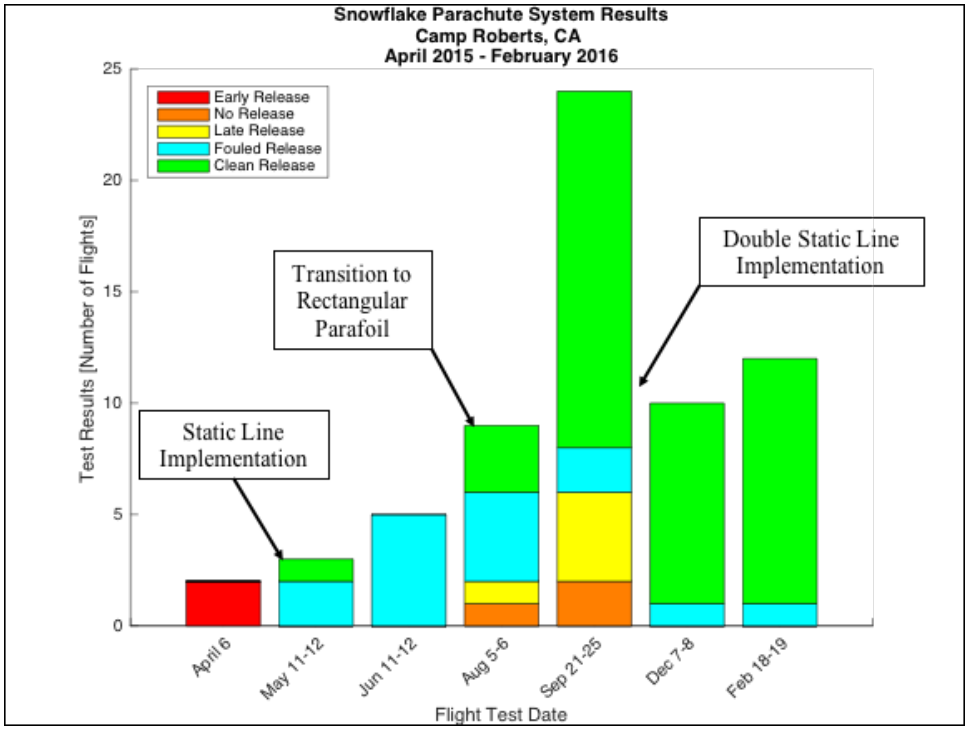

Figure 30. Failure Analysis of Snowflake Parachute Deployment Methods

The results of the August and September 2015 flight tests were successful in that they demonstrated a slight improvement in the likelihood of a clean parachute release when using the rectangular parafoil. Unfortunately, the flight tests revealed a previously unidentified problem with the parachute bag failing to open during freefall. As constructed, the design required sufficient drag to open the parachute bag and release the parachute. However, due to the design changes incorporated following the April 2015 tests to reduce the risk of parachute pre-deployment during the flight to release altitude, the parachute bag was now unable to provide a consistent opening. The bag had been constructed to survive a roughly 10-minute flight to release altitude at airspeeds approaching 50 knots. Even when the static release pin was pulled during the release, there was an insufficient drag force to open the parachute bag. Frequently, the Snowflake

would free-fall for close to 1500 feet before opening. When the parachute did release at these free-fall airspeeds, the associated opening shock caused significant stress on the internal components of the Snowflake as well as on the connecting hardware. During the August and September 2015 flight-testing, the parachute bag failed to open three times, each resulting in a ballistic profile terminating in complete disintegration on impact. The images shown in Figure 31 reveal some of the parachute malfunctions that plagued the single static release pin implementation. Of the 32 flight tests conducted with the static release pin design, only seven yielded a parachute that was fully inflated and controllable.

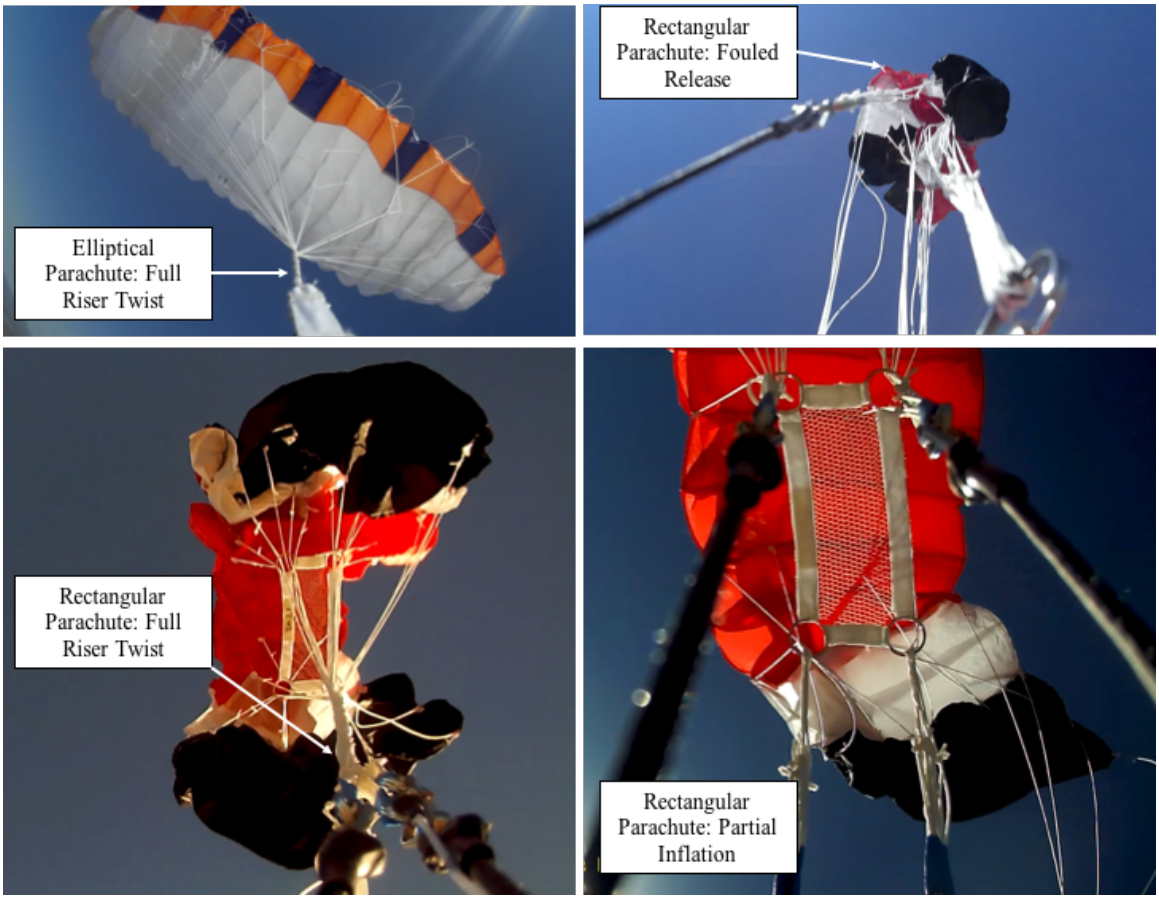

Figure 31. Representative Parachute Malfunctions Using Single Static Line Release Pin

As a result of the previously described inability to separate from the launch platform and deploy a parachute in a manner supporting control, the double static line deployment sequence was implemented during field testing in September 2015. The

sequence did have a few variations in development, but converged on the design discussed in Chapter IV. Results for the double static line deployment sequence demonstrated consistent performance by yielding a parachute deemed suitable for control in 29 of 31 flight experiments. Additionally, the two failures of the double static line sequence were fouled releases not representing the hazardous conditions produced by previous designs.

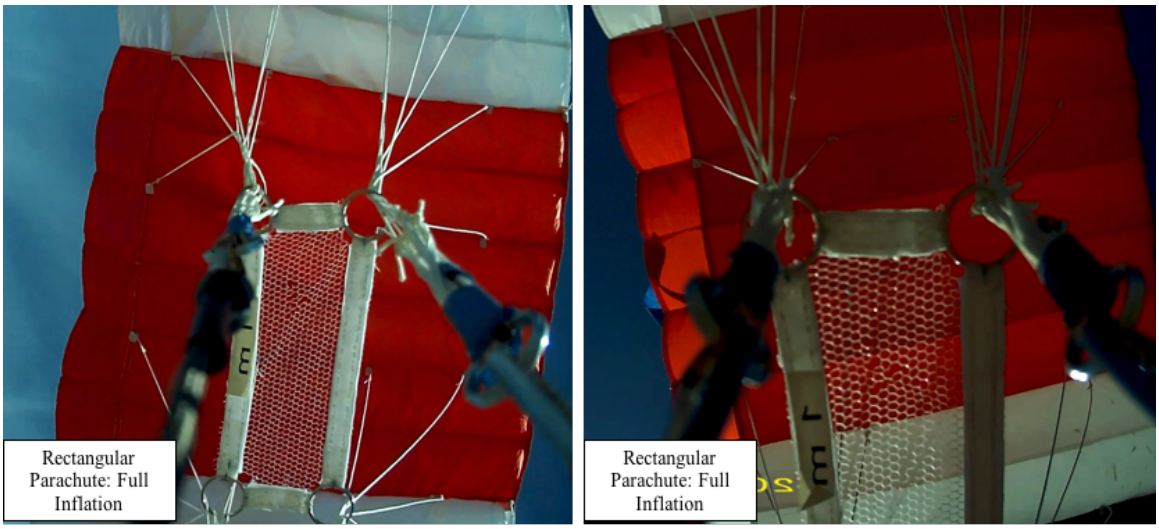

Figure 32. Representative Successful Parachute Inflations Using Double Static Line Deployment Sequence

2. Support for Experimental Data Collection

Given that the parachute sequence had begun to demonstrate relatively consistent and successful results, the author's design emphasis began to shift to analysis of the data being collected by the Pixhawk autopilot in September and December 2015. As shown in Table 6 and Figure 33, the Pixhawk autopilot proved unreliable in sensing, preserving and recording the experimental flight data required for control and navigation. Though various lab and flight experiments were attempted, the author was never able to isolate the fundamental causes of the failure to capture flight data. The author determined that the complex series of sensors required to conduct a flight experiment needed to be powered and functioning appropriately for the autopilot to remain armed and recording data. The most likely cause was repeated high magnitude deceleration, experienced on

either ground impact or in high velocity parachute deployment. Any transient interruption in the power supply or telemetry link could cause the Pixhawk to change flight modes and negatively impact its ability to record and preserve data.

Table 6. Summary of Autopilot Data Collection Results

Autopilot	No Data Recorded		Data Invalid		Data Valid		Total
	Number of Flights	% of Total	Number of Flights	% of Total	Number of Flights	% of Total	
Pixhawk	24	45.3%	10	18.9%	19	35.8%	53
X-Monkey	0	0.0%	0	0.0%	12	100.0%	12
Totals	24	36.9%	10	15.4%	31	47.7%	65

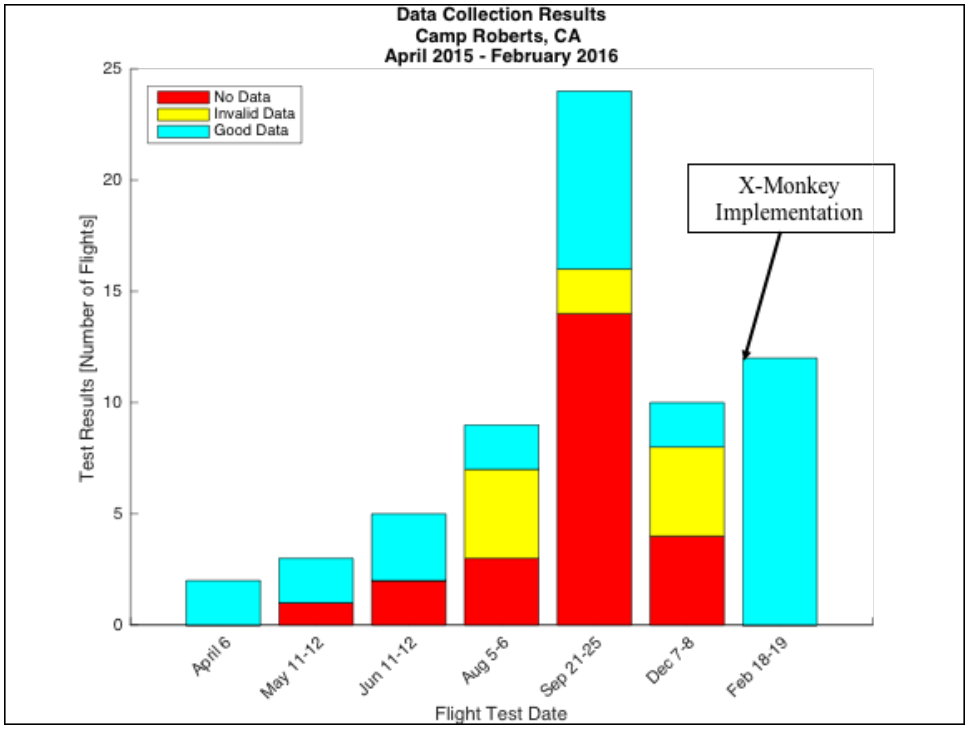

Figure 33. Summary of Autopilot Data Collection Results

In addition to the failure to record useful data, the Pixhawk was also subject to multiple small sensor component failures that would cause gross errors in the information being recorded. These failures were often undetectable during pre-flight programming They would only manifest themselves on subsequent data analysis revealing inaccurate

magnetic heading, altitude or GPS position information. As a result of this inability to adequately record experimental data, the author determined it was not suitable for use in the Snowflake platform and replaced it with the previously described X-Monkey which demonstrated significant improvement in reliability and consistency. In contrast to the Pixhawk recording valid data on 35.8% of its test flights, the X-Monkey has demonstrated 100% success in collecting and preserving flight data through 12 flight experiments.

B. COORDINATE TRANSFORMATION AND FLIGHT PROFILES

This section details the homogeneous coordinate transformation used to convert the X-Monkey autopilot flight data to a more usable reference frame, including a description on the use of quaternions. Additionally, this section includes samples of sensor data from lab experiments as well as representative flight data from a controlled Snowflake flight experiment.

1. Coordinate Transformation

Positioning the X-Monkey inside the Snowflake required performing a coordinate transformation to convert effectively the recorded sensor data, which was expressed in the sensor frame $\{s\}$, to the body coordinate frame $\{b\}$ for the Snowflake. The rotation matrix (R) shown below represents the orientation rotation of the X-Monkey sensor to the Snowflake body frame in terms of the Euler angles (φ, θ, ψ) required to rotate the coordinate frame. The Euler angles for the X-Monkey to Snowflake rotation matrix are shown in Figure 34.

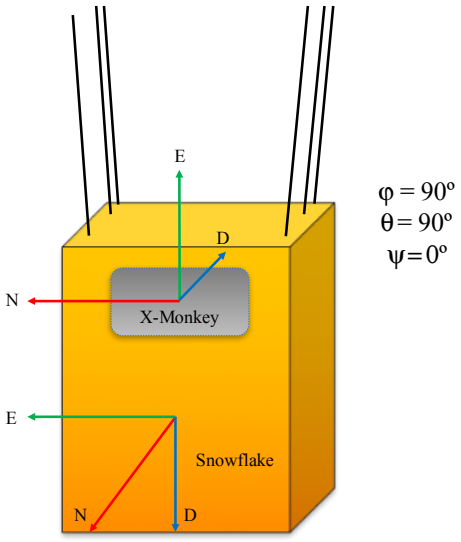

Figure 34. Coordinate Frame Relationship Between X-Monkey Sensor Frame and Snowflake Body Frame

$$ {}^{b}_{s}R = \begin{bmatrix} \cos\psi\cos\theta & \sin\psi\cos\theta & -\sin\theta \\ \cos\psi\sin\theta\sin\varphi - \sin\psi\cos\varphi & \sin\psi\sin\theta\sin\varphi + \cos\psi\cos\varphi & \cos\theta\sin\varphi \\ \cos\psi\sin\theta\cos\varphi + \sin\psi\sin\varphi & \sin\psi\sin\theta\cos\varphi - \cos\psi\sin\varphi & \cos\theta\cos\varphi \end{bmatrix} $$

$$ {}^{b}_{s}R = \begin{bmatrix} \cos(0^\circ)\cos(90^\circ) & \sin(0^\circ)\cos(90^\circ) & -\sin(90^\circ) \\ \cos(0^\circ)\sin(90^\circ)\sin(90^\circ) - \sin(0^\circ)\cos(90^\circ) & \sin(0^\circ)\sin(90^\circ)\sin(90^\circ) + \cos(0^\circ)\cos(90^\circ) & \cos(90^\circ)\sin(90^\circ) \\ \cos(0^\circ)\sin(90^\circ)\cos(90^\circ) + \sin(0^\circ)\sin(90^\circ) & \sin(0^\circ)\sin(90^\circ)\cos(90^\circ) - \cos(0^\circ)\sin(90^\circ) & \cos(90^\circ)\cos(90^\circ) \end{bmatrix} $$

$$ {}^{b}_{s}R = \begin{bmatrix} 0 & 0 & -1 \\ 1 & 0 & 0 \\ 0 & -1 & 0 \end{bmatrix} $$

The rotation matrix (R) was also converted to a quaternion vector (Q) to aid in post-flight processing as well as to facilitate implementation into the X-Monkey operating software, which internally utilized quaternions. Though the data outputted by the X-Monkey is in its native sensor frame, there is a series of internal routines that incorporate and utilize quaternion rotation sequences. The author expects that Lieutenant

Commander O'Brian will be able to implement the quaternion rotation sequences to develop further the control and navigation algorithms.

$$q_0 = \frac{\sqrt{1+tr\left({}^{b}_{s}R\right)}}{2} = \frac{\sqrt{1+0}}{2} = 0.5$$

$$q_1 = \frac{R_{23} - R_{32}}{4q_0} = \frac{0-(-1)}{4(0.5)} = 0.5$$

$$q_2 = \frac{R_{31} - R_{13}}{4q_0} = \frac{0-(-1)}{4(0.5)} = 0.5$$

$$q_3 = \frac{R_{12} - R_{21}}{4q_0} = \frac{0-(1)}{4(0.5)} = -0.5$$

$${}^{b}_{n}Q = \begin{bmatrix} q_0 \\ q_1 \\ q_2 \\ q_3 \end{bmatrix} = \begin{bmatrix} 0.5 \\ 0.5 \\ 0.5 \\ -0.5 \end{bmatrix}$$

Similarly, the same coordinate transformation was applied to the X-Monkey Euler angle rates ($\dot{\varphi}$), ($\dot{\theta}$) and ($\dot{\psi}$) to transform the values to Snowflake Euler angle rates in post-flight processing.

2. Lab Testing

To confirm the correct operation of the quaternion operator identified earlier, the author conducted a series of laboratory experiments. In each experiment, an X-Monkey was installed as shown in Figure 34 and multiple scripted experiments were conducted. Primarily, the Snowflake was rotated 360 degrees of positive pitch, 360 degrees of positive roll and 360 degrees of positive yaw. The experiment took approximately 30 seconds to complete and included downloading the experimental data file from the X-Monkey and importing into MATLAB for processing using one of the scripts shown in the Appendix. Representative results from an experiment are shown in Figures 35 and 36.

The Euler angle data were adjusted in MATLAB to convert the output angles from the X-Monkey to a more useful range. The range of roll angles was converted to +/-

180 degrees, the pitch angles were converted to +/- 90 degrees and the yaw angles were converted to a range from 0–360 degrees using the `wrapTo180` function in MATLAB. The roll and yaw transients exhibited in Figure 35, which occurred during the 360-degree positive pitch rotation, were expected variations associated with a 90 degree pitch up/pitch down orientation.

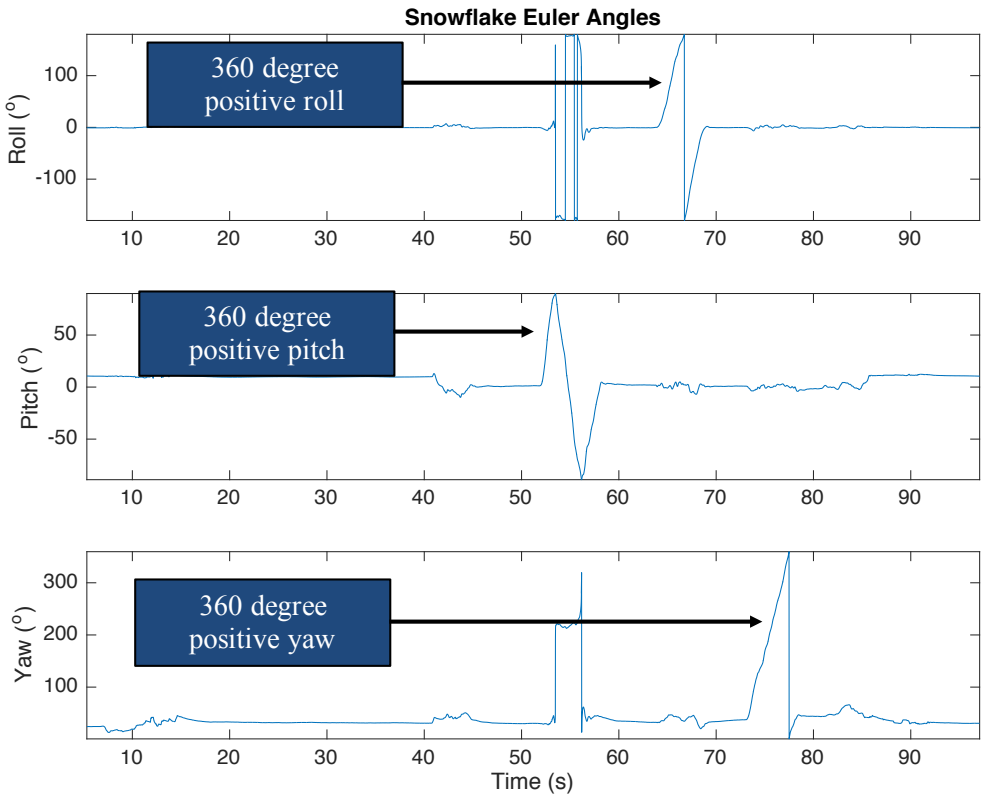

Figure 35. Lab Experiment Results: Snowflake Euler Angles following Coordinate Transformation

Additionally, the Euler angle rates recorded during this experiment were also shifted from the X-Monkey orientation to the more appropriate Snowflake orientation as shown in Figure 36. The raw sensor output data were filtered using a one dimensional median filter function (`medfilt1`) in MATLAB to reduce some of the high frequency noise in the rate sensors and to make the experimental output a bit more intuitive.

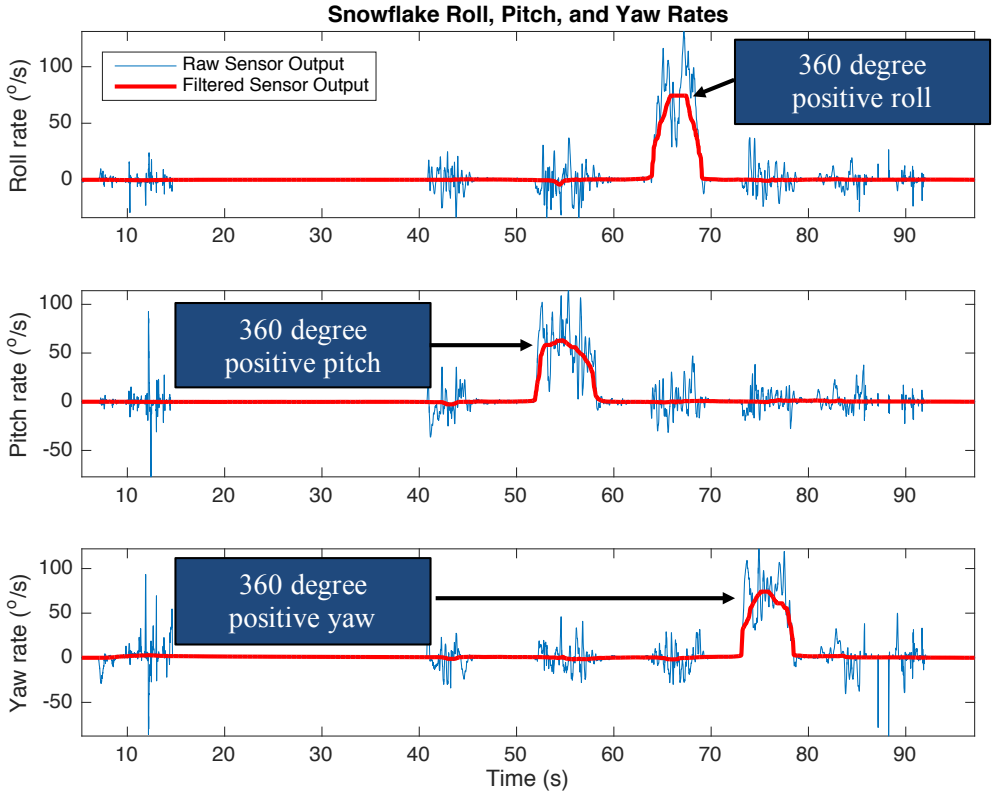

Figure 36. Lab Experiment Results: Snowflake Euler Angle Rates following Coordinate Transformation

3. Flight Tests

From February 18–19, 2016, 12 live flight experiments were conducted at McMillan Airfield, Camp Roberts, CA utilizing the Snowflake ADS with an installed X-Monkey. Each of these flights utilized the double static line release sequence, with 11 of 12 flights resulting in a full canopy inflation. The one failure was attributed to a snag in the parachute support lines when utilizing a spreader, which was subsequently removed. Comprehensive post-flight data analysis was conducted to gain insight into the dynamics associated with launch, separation from releasing aircraft and steady state autonomous flight. In each of these experiments, the control line retraction was systematically varied to induce a heading change in the platform. This data was to be utilized to construct a SISO model of the Snowflake for subsequent control system design. The principal objectives of these tests were to validate the airframe separation mechanism and to

collect meaningful data on the flight profile. Both of which were achieved. The data shown in Figures 37 through 42, are from a single flight which was representative of each of the 12 flight experiments. In this particular example, the Snowflake was programmed with a two-centimeter retraction of the right control line to induce a positive yaw.

A bird's-eye view of the GPS position of the Snowflake is shown in Figure 37 shortly after release from the launch aircraft at an altitude of approximately 2,000 above ground level (AGL). As the double static line sequence was utilized, the Snowflake release and parachute deployment occurred nearly simultaneously. The author defined a steady state period of autonomous Snowflake flight beginning five seconds after parachute deployment to five seconds before touchdown. This helped in isolating the dynamics and oscillations associated with parachute release. The flight control program is designed to actuate following this transient condition and provide guidance to the pre-programmed destination. The isolation of the five seconds prior to touchdown was done to facilitate scaling during data analysis as the transients on landing tended to mask the steady state flight characteristics.

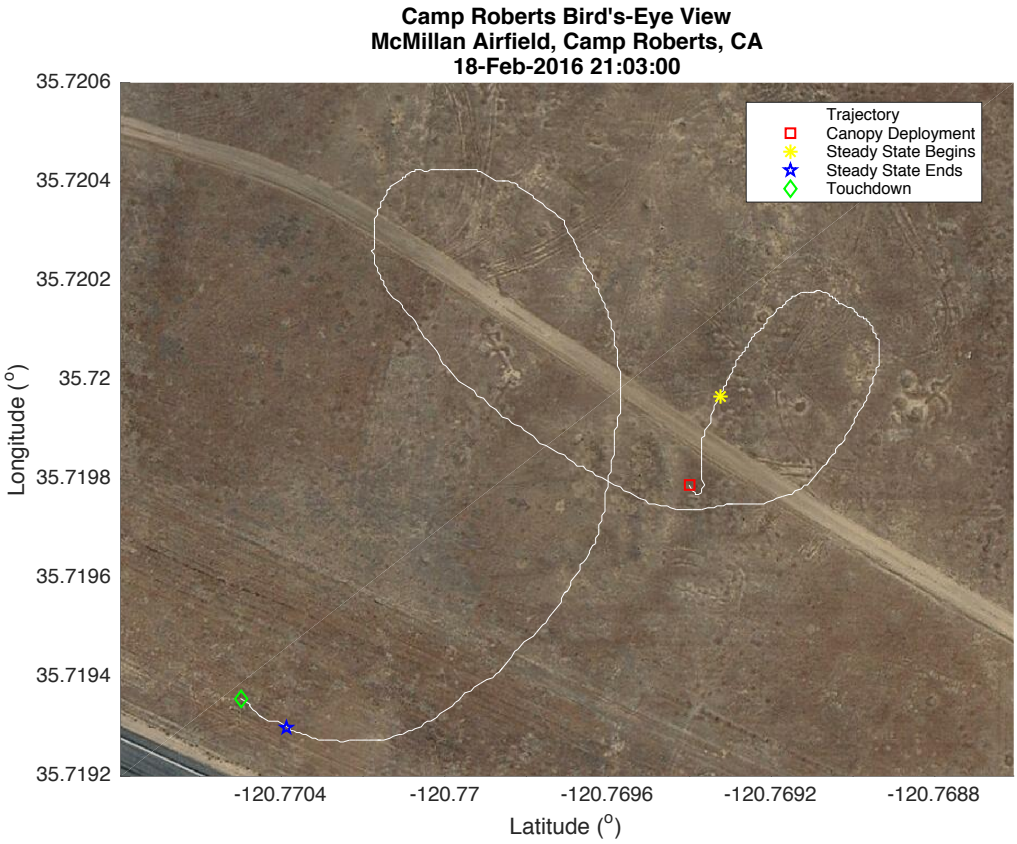

Figure 37. Flight Test Results: Bird's-Eye View

The same flight experiment is represented three-dimensionally in Figure 38. The canopy deployment, steady state definitions and touchdown points are all shown. Additionally, the flight profile is displayed using sensor input from the X-Monkey barometric altimeter as well as the altitude reported from the internal GPS. In this example, there is a distinct difference between the two, but a comprehensive analysis of all test results demonstrated significant unreliability in the accuracy of the GPS position and altitude. Until the source of the GPS instability can be isolated, usage of the barometric altimeter is recommended. Additionally, analysis of the discrepancy between the two altitude sensors will be required to determine precise estimate of the above ground level (AGL) altitude in order to refine terminal control and accuracy.

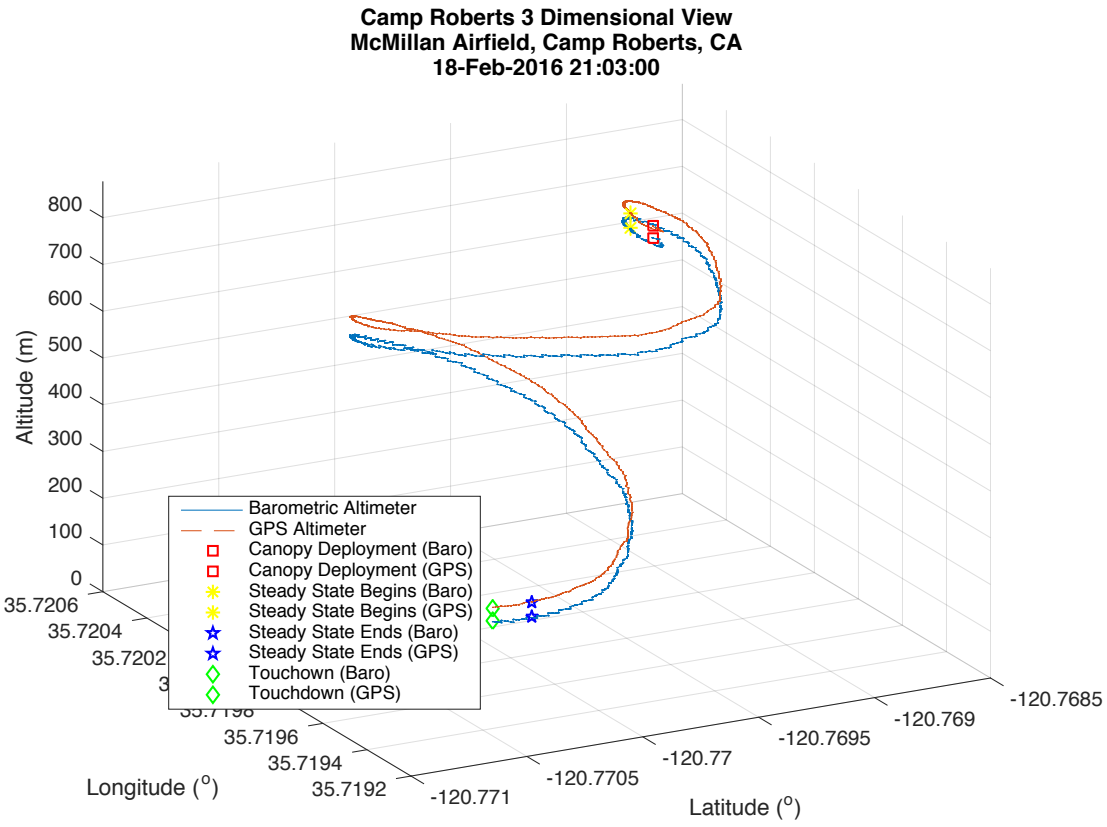

Figure 38. Flight Test Results: Three-Dimensional View

More data from this flight experiment are shown in Figure 39, which shows a clear delineation of the three separate elements of the flight, additional levels of detail in the GPS sensor as well as the magnitude of total acceleration recorded by the three-axis accelerometers within the X-Monkey. The top plot of the altitude profile is combined with the second plot of total acceleration to define significant flight events for data analysis. The acceleration spikes at approximately 350 seconds, 630 seconds and 750 seconds, represent the catapult launch of the UAV, the release of the Snowflake ADS and the impact with the ground. Various other conditions were investigated, but the total acceleration was deemed most reliable in isolating these significant flight events. Additionally, in the top plot of Figure 39, the erroneous altitude reported by the GPS sensor is shown.

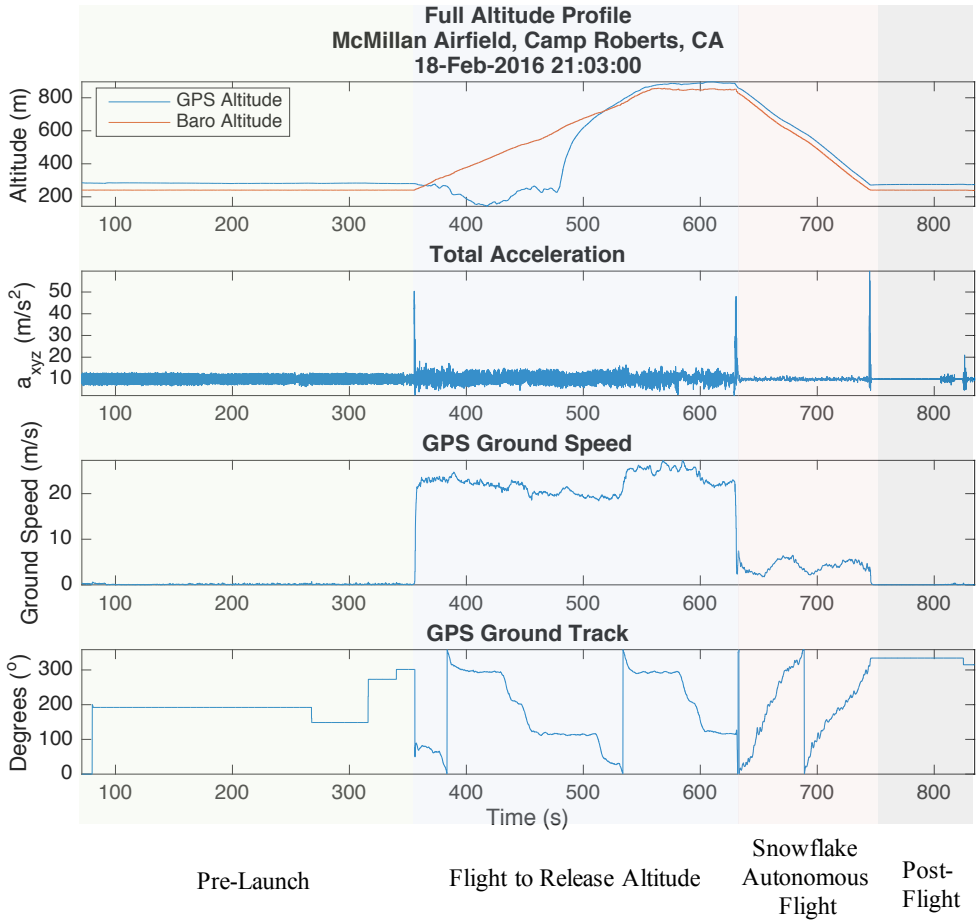

Figure 39. Flight Test Results: Altitude Profile, Total Acceleration and GPS Ground Speed/Track

The Snowflake autonomous flight segment is expanded in Figure 40 to reveal the individual components of the velocity as reported by the GPS in the X-Monkey. The north and east components (V_N and V_E) are shown in the top plot, the down component (V_D) in the second plot and the composite ground track velocity component (V_G) in the bottom plot. The ground velocity was calculated in post-flight processing using the following expression:

$$V_G = \sqrt{(V_N)^2 + (V_E)^2}$$

The mean values for the down and ground component velocities, (V_D) and (V_G), respectively, were calculated and are shown in Figure 40 as well. The ground velocity value (V_G) is useful for completing real time wind estimation, though the X-Monkey will

need an installed onboard airspeed sensor in subsequent design iterations if this functionality is to be implemented successfully. Providing there is little or negligible vertical wind component, the GPS vertical velocity component (V_D) is sufficiently accurate to facilitate flight path prediction and glideslope management in the terminal phase.

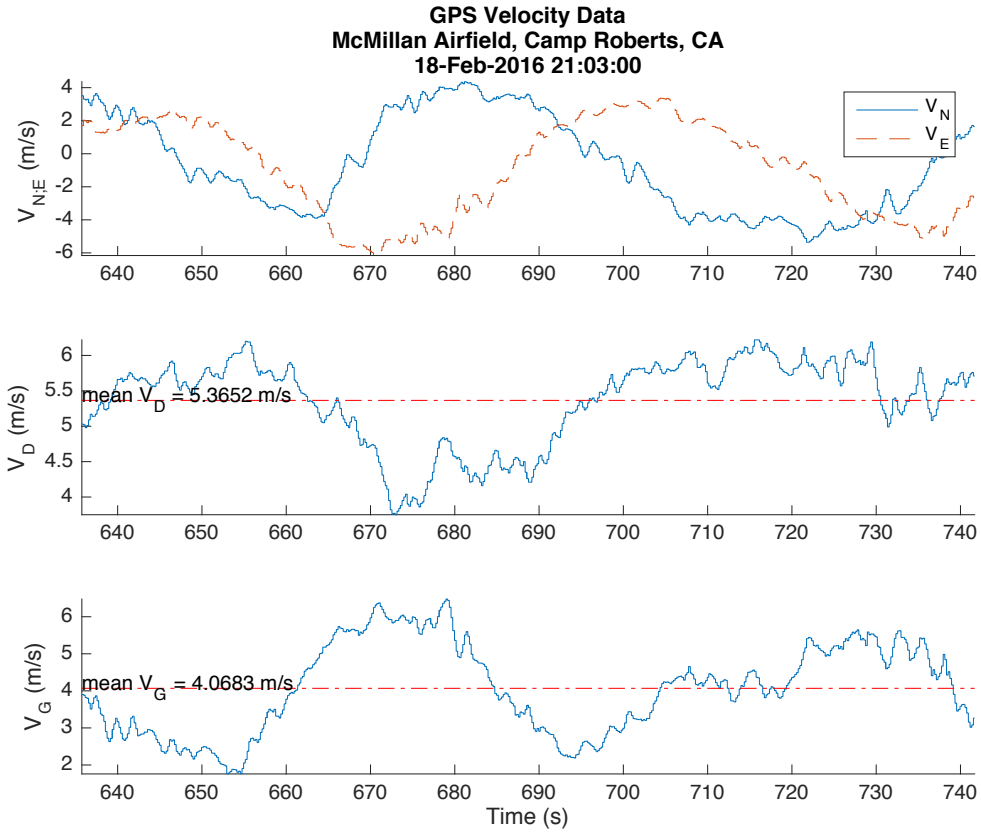

Figure 40. Flight Test Results: Snowflake Autonomous Flight GPS Velocity Components

The Euler orientation of the Snowflake during this autonomous flight segment is shown in Figure 41. Unfortunately, the data shown highlight a problem with the magnetic calibration of the X-Monkey that manifested itself in flight-testing. The hardware version of the X-Monkey had an internal software error that has since been corrected. The magnetic calibration reference vector was not being saved correctly, which produced the erroneous yaw angles represented in the data. From the flight path reconstruction data presented

earlier in Figures 37 and 38, the Snowflake executed two right 360-degree rotations about the yaw axis, but the recorded Euler headings are within a range of 75 to 150 degrees.

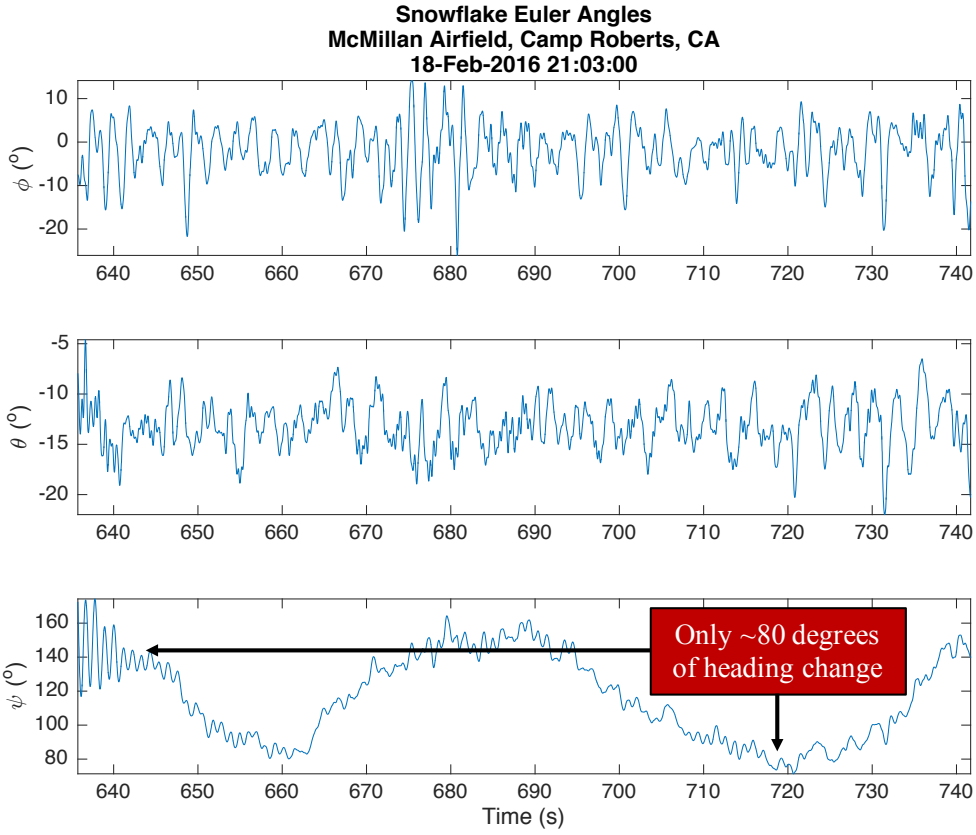

Figure 41. Flight Test Results: Snowflake Euler Angles

Figure 42 shows an expanded comparison of the Euler yaw heading and the GPS ground track during the period of autonomous Snowflake flight. Again, the erroneous heading information is shown, but this comparison is expected to be useful for conducting a real-time wind estimation. The magnetic reference vector calibration error has subsequently been corrected, and the correct Euler orientations have been verified correct in a series of lab experiments conducted in the ADSC lab.

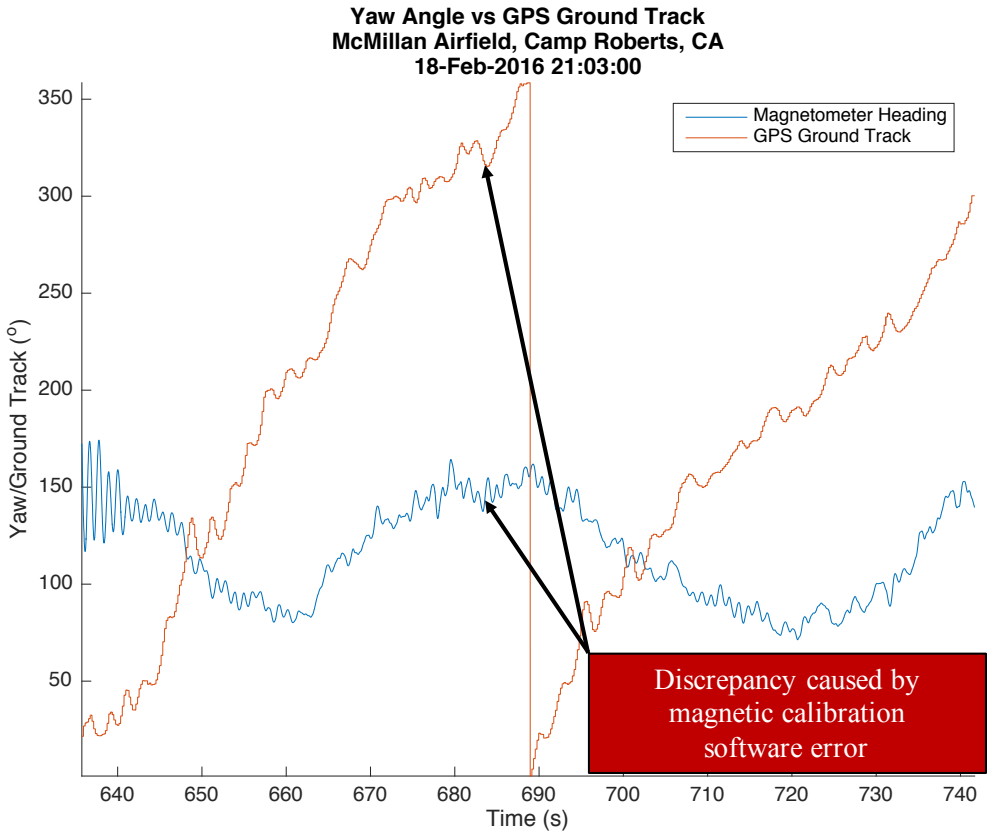

Figure 42. Flight Test Results: Snowflake Yaw Angle versus GPS Ground Track

Finally, a representative flight sequence of the Snowflake ADS is shown in Figure 43. This sequence is a compilation of several flights showing the diverse nature of the experiments. The Snowflake ADS was successfully employed from two different types of UAVs, utilized three uniquely developed separation sequences, incorporated two different autopilot computers and collected experimental data from autonomous as well as radio controlled back-up modes. The data collected and the methods for analysis are presented to assist future research endeavors in refining the control and guidance algorithms to enhance terminal accuracy.

Figure 43. Compiled Snowflake ADS Test Sequence

C. SUMMARY

This chapter compiled the 65 flight tests conducted over a nearly ten-month period, as well as several simulations conducted in the ADSC laboratory at NPS. The results from the flight tests are correlated with sequential improvements in the parachute deployment methods that were derived from failure mode analysis. Additionally, the ability of each autopilot to capture and retain valid experimental data is described, as it directly influenced the author's conversion from the Pixhawk to the X-Monkey flight computer. Once successful flight data was recorded, this chapter detailed various lab simulations and the mathematics used to convert recorded data to a more useful coordinate frame using quaternions. Subsequently, a representative flight profile is described and illustrated to facilitate follow-on control system development. The results from these flight and computer simulations are used to derive several conclusions relating to the viability of COTS technology to produce low-cost micro-light weight PADSs that can provide additional capability to the battlefield.

VI. CONCLUSION AND RECOMMENDATIONS

A. CONCLUSION

Based on theoretical analysis and assessment of the flight-test results, the author's overall conclusion is that low-cost, COTS navigation components are likely to provide sufficient accuracy and reliability to close the capability gap between the PADSs currently in operation and the combat operational need for rapid-response, tactical logistical resupply in austere and dispersed locations. More research is needed to provide conclusive evidence as to the economic viability of a highly accurate, purpose built micro-light weight class PADSs when contrasted with potential multiple use alternatives.

In addition to the above conclusion, several additional conclusions are offered to address the secondary research objectives. Operational limitations for employment are discussed as well as several conclusions derived from the application of systems engineering methodologies to the construction of several initial prototypes and the completion of a technical research effort at NPS.

1. Operational Employment Limitations of Micro-Light Weight PADSs

The accuracy of the Snowflake ADS is still being developed and enhanced, however this research effort has realized some potential shortcomings associated with operational employment. Micro-light weight PADSs have an inherent requirement to be small and inexpensive to alleviate the warfighter from being required to retain and return the PADS for reuse. If the cost or complexity associated with a micro-light weight PADS grows to the point where it can no longer be considered disposable, then it becomes questionable as to whether a PADS is the preferred method for logistical delivery. Only in the specific case when long-range resupply is required, is a PADS able to outperform a small package delivered via more conventional vertical takeoff and landing UAS, such as a quad copter.

As this research uncovered, the cost to commercially procure a single rectangular ram-air parachute is approximately $400. Viable economy of scale production will most assuredly reduce the cost to construct a ram-air parachute with sufficient build quality to

support failure rate reduction. Though this research did not include a full cost analysis to procure a developed system, cost efficiency must be balanced with the requirement for increased terminal accuracy. As the burdening of a tactically engaged warfighter with the responsibility to return a purpose-built ram-air parachute is undesirable, continued improvements in micro-light PADSs must be implemented in a manner which retains the attribute of being a single-use item.

This conclusion was reached as a result of the application of the systems engineering methodology to research and understand the core user/stakeholder needs and resultant requirements. The need demonstrated by the hypothetical user in most CONOPS, is for logistical resupply, not for logistical resupply via PADS. As such, the systems engineering methodology was an effective tool in the development of the Snowflake ADS in that it had to be the best approach to meeting the core stakeholder needs.

2. Application of Systems Engineering Methodology

Traditional and Agile methodologies were critical tools in the conceptual and preliminary design of a micro-light weight class PADS. The ability to rapidly respond to failures, identify root causes and incorporate multiple design changes though iteration was critical in development. Additionally, the ability to identify emerging user/stakeholder needs and rapidly iterate accordingly was instrumental to the success that was achieved. Lastly, the application of various design thinking principles to identify solutions based on desired functionality enhanced development when contrasted to component specific solutions.

3. Prototype Design for Operational as Compared to Developmental Objectives

Though the systems engineering principles identified earlier were instrumental in design, there were some identified shortfalls in a design focused purely on the end users specified needs. Analysis of stakeholder needs was crucial and valuable, but it did not necessarily produce an effective “Big Design Up Front” in the conceptual and preliminary design phases. The number of design iterations required simply to support

developmental testing was significant. As such, it was necessary to identify additional effective needs for various phases of development in order to successfully design a prototype suitable for operational employment.

4. Integration of Multi-Domain NPS Engineering Curriculum

The most rewarding aspect of this research endeavor has been the ability to engage with engineering faculty and students outside of the Systems Engineering Department at NPS. The author believes that the quantity and quality of learning was magnified significantly through the application of the systems engineering methodology to an ongoing engineering project, commencing with initial design and culminating with field experimentation. This research has allowed the author to investigate robotic fundamentals, unmanned systems navigation systems and classic control while designing and integrating a complete PADS.

In contrast, the author strongly believes that the application of systems engineering toward an abstract or theoretical problem is counterproductive. Systems engineering education must include the application of concepts toward a complex applied engineering effort. Failure to do so is a disservice to the both the system engineer and the teams of domain specific engineers. The author frequently observed how a domain specific engineer could focus on a specific solution and lose sight of the broader functionality that was trying to be achieved. The systems engineering methodology was useful in this regard. In contrast, an abstract systems engineer who lacks a basic understanding of the underlying engineering complexity associated with design and testing lends little to the project.

5. Continuity and Documentation of Research Effort

The author began this research endeavor with the intention of improving the results of previous students. Unfortunately, the lack of continuity in the project contributed greatly to the overall complexity and difficulty. The author spent close to nine months getting the research platform back to the level of capability where it was a few years ago. As software and hardware are revised continually, the period of viability associated with the equipment in any research project is much shorter than expected. For

the Snowflake ADS, or any research project to continue to evolve and improve, there must be a continuous supply of students or laboratory technicians who are familiar with the technical specifications of the project.

B. RECOMMENDATIONS FOR TECHNICAL IMPROVEMENTS

The recommendations provided are a small sample of the technical areas in which the Snowflake ADS prototype could be improved to enhance its navigational accuracy and associated operational utility. As the final prototype is suitable for subsequent scientific experimentation, significant room for improvement exists before the utility of a micro-light weight class PADS can be fully explored in an operational setting.

1. Guidance and Control Algorithms

The parallel effort of Lieutenant Commander O'Brian to implement a guidance and control algorithm into the X-Monkey autopilot is a significant undertaking, but necessary for the development of autonomous navigation. Due to the earlier described failures in the preliminary design, the author was not able to collect comprehensive data to assist in developing a SISO model linking control line retraction to Snowflake yaw angle. The late transition from the Pixhawk autopilot to the X-Monkey autopilot contributed to the latency in developing a control algorithm as the two autopilots are programmed completely differently.

In addition to the SISO control line retraction to yaw rate model, a multiple input multiple output (MIMO) model can be created to simultaneously control the yaw, provide some measure of roll damping during the descent as well as offer pitch response to accommodate changes in forward velocity. The dual input associated with independent actuation of the left and right control lines can be used to examine a variety of outputs through the use of state space design techniques.

2. Robustness of GPS Navigation Solution

Experiments conducted using the X-Monkey demonstrated some small reliability inconsistencies with the GPS sensor data. Due to the relatively low power of a received GPS signal and the internally mounted X-Money, future design iterations must include

the external GPS antenna to boost signal reception. If the external antenna does not provide the necessary additional signal strength, then a pre-flight verification of GPS signal strength is necessary prior to experimentation. As the X-Monkey can be expected to sustain a roughly 5 G impact on landing, the veracity of the navigation solution must be confirmed prior to follow-on experimentation.

3. Wind Estimation

To enhance the accuracy of the Snowflake ADS, the AGU must be able to measure and refine real-time wind speed and direction. The integration of an externally mounted airspeed sensor to the X-Monkey was considered, but not implemented in the course of this research due to insufficient time and available flight-testing. External airspeed sensors increase the risk for parachute tangles/malfunctions on deployment and are unlikely to have the precision required for low-airspeed flight and wind estimation with rapidly changing platform orientation. One of several potential wind estimation maneuvers could be completed during descent and incorporated into the guidance and control algorithms. These methods are designed to measure and adjust to a continually changing wind profile during platform descent and offer precision that an airspeed sensor is unlikely to provide in a low-speed dynamic flight envelope.

4. Improved Parachute Design

This research effort commenced with the objective of assessing the potentially enhanced maneuverability of elliptical ram-air parachutes with regard to micro-light weight class PADSs. Unfortunately, the manufacturing quality of the elliptical parachutes was not sufficient to support experimentation. However, the question remains as to whether the elliptical parachutes can offer greater maneuverability and the potentially resultant increase in terminal accuracy. If a ram-air parachute becomes available, the Snowflake ADS is still a viable test platform to support more exhaustive examination of its flying qualities.

5. Incorporation of an Imaging Sensor

Previous versions of the Snowflake ADS had limited integration of a monocular vision sensor to assist in the acquisition of a non-cooperative mobile target and navigation in the GPS-denied environment. Unfortunately, the author was not able to incorporate a vision sensor, due to the late transition to the X-Monkey platform. Though an imaging sensor could assist in the terminal phase of a precise delivery for a mobile target, it could also assist in pose estimation in a GPS denied or degraded environment. As such, the incorporation of an imaging sensor does potentially increase the technological and cost complexity past the threshold for operational feasibility for a micro-light weight class PADS. Notwithstanding, the concept is still potentially viable to augment terminal accuracy for larger PADSs that are not considered to be single use items, especially in the GPS denied environment.

APPENDIX. MATLAB SCRIPTS

A. FUNCTION TO CONVERT SENSOR DATA TO BODY FRAME

This function was used multiple times in analysis of both laboratory experiments and flight data to convert the Euler orientation of the X-Monkey sensor to a more useful Euler orientation of the Snowflake.

```
function [SFeul] = XMeul2SFeul(eul)

%This function accepts user input of a [1x3] vector of Euler angles in
%degrees. Input Euler angles [roll pitch yaw]. This rotates the Euler
%angles output from X-Monkey to the Snowflake orientation. Use to
%convert raw X-Monkey data to generate flight profile of SF. Since X-
%Monkey outputs roll in 0—360, and yaw in 0—360, this function wraps
%the data to roll=+/-180 and yaw=+/-180 for computation. Output wraps
%the yaw to 0—360 for heading output.

eul=wrapTo180(eul);
qM_I=eul2quat(eul);
qI_S=[0.5 0.5 0.5 -0.5]';
qM_S=q_mult(qM_I,qI_S);
SFeul(1)=atan2(2*(qM_S(3)*qM_S(4)+qM_S(1)*qM_S(2)),
               (1-(2*(qM_S(2)^2+qM_S(3)^2))));

SFeul(2)=-asin(2*(qM_S(2)*qM_S(4)-qM_S(1)*qM_S(3)));

SFeul(3)=atan2(2*(qM_S(2)*qM_S(3)+qM_S(1)*qM_S(4)),
               (1-(2*(qM_S(3)^2+qM_S(4)^2))));

SFeul=rad2deg(SFeul);
SFeul(3)=wrapTo360(SFeul(3));
end
```

B. SCRIPT TO ANALYZE LABORATORY ORIENTATION EXPERIMENTS

This script was used to rotate, analyze and confirm the correct orientation of the Euler data recorded by the X-Monkey to the more appropriate Snowflake frame for use in subsequent flight-testing. It utilizes the Euler angle conversion function created separately.

```
% Snowflake X-Monkey Data Processing
close all; clear all; clc;
%% Read in the data file you want to process that include YMDHM
%sequence:
```

```
%Note: This takes an X-Monkey CSV file which must be generated using
%the PARSR Program. Add the 4-digit year to the beginning of the data
%file name.

[filename, pathname] = uigetfile('*.csv','Choose First X-Monkey data
file');
FileName = [pathname filename];
iD=strfind(filename,'201');
YY=str2num(filename(iD:iD+3));     Mo=str2num(filename(iD+4:iD+5));
DD=str2num(filename(iD+6:iD+7));   HH=str2num(filename(iD+8:iD+9));
Mi=str2num(filename(iD+10:iD+11));
DateNumber0=datenum(YY,Mo,DD,HH,Mi,0);
DateString = datestr(DateNumber0);
File = csvread(FileName,1,0);

choice = questdlg('Would you like to enter another file from this
experiment?','Additional Files');
YN=strcmp(choice,'Yes');

while YN == 1
      [filename, pathname] = uigetfile('*.csv','Choose Another X-Monkey
data file');
      FileName = [pathname filename];
      File = vertcat(File,csvread(FileName,1,0));
      choice = questdlg('Would you like to enter another file from this
experiment?',...
      'Additional Files');
      YN=strcmp(choice,'Yes');
end

eul=[File(:,28) File(:,29) File(:,30)];
[M, N]= size(eul);
SFeul = zeros(M,N);
for i=1:M
SFeul(i,:)=XMeul2SFeul(eul(i,:));
end

%% Create Plot of X-Monkey Roll, Pitch, and Yaw
figure(1)
subplot(311)
plot(File(:,5),File(:,28))
title('X-Monkey Euler Angles');
ylabel('Roll (^o)');
axis tight

subplot(312)
plot(File(:,5),File(:,29))
ylabel('Pitch (^o)');
axis tight

subplot(313)
plot(File(:,5),File(:,30))
ylabel('Yaw (^o)');
xlabel('Time (s)');
axis tight
```

```
%% Create Plot of Roll, Pitch, and Yaw
figure(2)
subplot(311)
plot(File(:,5),SFeul(:,1))
title('Snowflake Euler Angles');
ylabel('Roll (^o)');
axis tight

subplot(312)
plot(File(:,5),SFeul(:,2))
ylabel('Pitch (^o)');
axis tight

subplot(313)
plot(File(:,5),SFeul(:,3))
ylabel('Yaw (^o)');
xlabel('Time (s)');
axis tight

%% Create Euler Rate Plots
figure(3)
subplot(311)
filterroll=medfilt1(-File(:,37),500);
plot(File(:,5),-File(:,37))
hold on
plot(File(:,5),filterroll,'r','LineWidth',2)
title('Snowflake Roll, Pitch, and Yaw Rates');
legend('Raw Sensor Output','Filtered Sensor
Output','Location','northwest');
ylabel('Roll rate (^o/s)');
axis tight
hold off

subplot(312)
filterpitch=medfilt1(File(:,35),500);
plot(File(:,5),File(:,35));
hold on
plot(File(:,5),filterpitch,'r','LineWidth',2);
ylabel('Pitch rate (^o/s)');
axis tight
hold off

subplot(313)
filteryaw=medfilt1(-File(:,36),500);
plot(File(:,5),-File(:,36));
hold on
plot(File(:,5),filteryaw,'r','LineWidth',2);
ylabel('Yaw rate (^o/s)');
xlabel('Time (s)');
axis tight
hold off
```

C. SCRIPT TO MERGE X-MONKEY .CSV FILES TO SINGLE .MAT FILE

This script was used to combine the series of .csv files that were outputted by the X-Monkey. Due to some hardware limitations internal to the X-Monkey, each output data file is only 7Mb. Following the experiment, the series of .csv files can be merged to a single .mat file to speed up analysis.

```
%% Script for merging multiple .csv files into a single.mat file
% First redefine the YYYYMMDDSF(#)D(Drop#).mat file at the end
% Import any number of .csv files, creates .mat file
% Move .mat file to appropriate folder

close all; clear all; clc

[filename, pathname] = uigetfile('*.csv','Choose First X-Monkey data
file');
FileName = [pathname filename];
iD=strfind(filename,'201');
YY=str2num(filename(iD:iD+3));      Mo=str2num(filename(iD+4:iD+5));
DD=str2num(filename(iD+6:iD+7));    HH=str2num(filename(iD+8:iD+9));
Mi=str2num(filename(iD+10:iD+11));
DateNumber0=datenum(YY,Mo,DD,HH,Mi,0);
DateString = datestr(DateNumber0);
File = csvread(FileName,1,0);

choice = questdlg('Would you like to enter another file from this
flight?','Additional Files');
YN=strcmp(choice,'Yes');

while YN == 1
      [filename, pathname] = uigetfile('*.csv','Choose Another X-Monkey
data file');
      FileName = [pathname filename];
      File = vertcat(File,csvread(FileName,1,0));
      choice = questdlg('Would you like to enter another file from this
flight?','Additional Files');
      YN=strcmp(choice,'Yes');
end
save 20160219SF4D3.mat    % Name .mat output file here
```

D. SCRIPT TO ANALYZE X-MONKEY FLIGHT TEST DATA

This script uses the .mat file created earlier to process that data and produce a series of graphs to analyze the flight profile.

```
%% Snowflake X-Monkey Data Processing using a .mat file
% This script uses a full .mat file from the flight
% User selects full flight file and processes accordingly
% CSV version merges the files and then processes
% To use this version, run the MergeFiles.m script once and
```

```
% Save the .mat file in the correct directory

close all;clear all;clc;

[filename, pathname]=uigetfile('*.mat','Choose X-Monkey .mat file');
fname=fullfile(pathname,filename);
load(fname);

%% Set Variables
Servo0neutral=1491;
Servo1neutral=1508;

%% Set Location
testsite='McMillan Airfield, Camp Roberts, CA';

%% Calculate Snowflake Release and Parachute Deployment
Tskip=0;
%[maxAlt,IndAlt]=max(File(:,22));     %Use GPS Altitude
[maxAlt,IndAlt]=max(File(:,52));      %Use Baro Altitude
Tskip=Tskip+IndAlt;
disp(['Release altitude ' num2str(maxAlt,3) ' m'])

% Use total acceleration to find launch, release and land
% View Figure (1) to determine what exact peaks represent and adjust
% Smaller data files may not have all three events
% Cross reference with altitude plots as well

Acceltot=sqrt(File(:,32).^2+File(:,33).^2+File(:,34).^2);
[pks,locs] = findpeaks(Acceltot, 'MINPEAKHEIGHT',
40,'MinPeakDistance',1000);

T20Launch=locs(1);
SFChuteDeploy=locs(2);
SFLand=locs(3);

%T20Launch=locs(2);
%SFChuteDeploy=locs(3);
%SFLand=locs(4);

ReleaseDelay=100*5; % Five second after release
LandCutoff=100*3;   % Three seconds prior to ground impact

%ChuteOpenAlt = File(SFChuteDeploy,22); %GPS Altitude
ChuteOpenAlt = File(SFChuteDeploy,52);  %Baro Altitude
%LandAlt=File(SFLand,22);          %GPS Altitude
LandAlt=File(SFLand,52);           %Baro Altitude

DropProfile = File(SFChuteDeploy:SFLand,:);
SSDropProfile=File(SFChuteDeploy+ReleaseDelay:SFLand-LandCutoff,:);
AltRange = ChuteOpenAlt - LandAlt;
DescentTime = File(SFLand,5)-File(SFChuteDeploy,5);

%% Convert X-Monkey Euler Angles to Snowflake Euler Angles
eul=[SSDropProfile(:,28) SSDropProfile(:,29) SSDropProfile(:,30)];
[M, N]= size(eul);
```

```
SFeul = zeros(M,N);
for i=1:M
SFeul(i,:)=XMeul2SFeul(eul(i,:));
end

%% Create Birds-Eye View Plot
figure(1)
hold on
plot(DropProfile(:,21),DropProfile(:,20),'w-')
plot(DropProfile(1,21),DropProfile(1,20),'rs')
plot(SSDropProfile(1,21),SSDropProfile(1,20),'y*')
plot(SSDropProfile(end,21),SSDropProfile(end,20),'bp')
plot(DropProfile(end,21),DropProfile(end,20),'gd')
plot_google_map('MapType','satellite');
title({'Camp Roberts Bird's-Eye View';testsite;DateString});
h=legend('Trajectory','Canopy Deployment','Steady State Begins',...
         'Steady State Ends','Touchdown','location','best');
set(h,'fontsize',8);
xlabel('Latitude (^o)'), ylabel('Longitude (^o)')
hold off

%% Plot 3D Profile
figure(2)
hold on

plot3(DropProfile(:,21),DropProfile(:,20),DropProfile(:,52),'-');
plot3(DropProfile(:,21),DropProfile(:,20),DropProfile(:,22),'--');
plot3(DropProfile(1,21),DropProfile(1,20),DropProfile(1,52),'rs')
plot3(DropProfile(1,21),DropProfile(1,20),DropProfile(1,22),'rs')
plot3(SSDropProfile(1,21),SSDropProfile(1,20),SSDropProfile(1,52),'y*')
plot3(SSDropProfile(1,21),SSDropProfile(1,20),SSDropProfile(1,22),'y*')
plot3(SSDropProfile(end,21),SSDropProfile(end,20),SSDropProfile(end,52)
,'bp')
plot3(SSDropProfile(end,21),SSDropProfile(end,20),SSDropProfile(end,22)
,'bp')
plot3(DropProfile(end,21),DropProfile(end,20),DropProfile(end,52),'gd')
plot3(DropProfile(end,21),DropProfile(end,20),DropProfile(end,22),'gd')

title({'Camp Roberts 3 Dimensional View';testsite;DateString});
legend('Barometric Altimeter','GPS Altimeter','Canopy Deployment
(Baro)',...
    'Canopy Deployment (GPS)','Steady State Begins (Baro)','Steady
State Begins (GPS)',...
    'Steady State Ends (Baro)','Steady State Ends (GPS)','Touchown
(Baro)','Touchdown (GPS)','Location','best');
xlabel('Latitude (^o)');
ylabel('Longitude (^o)');
zlabel('Altitude (m)');
zlim([0 inf])
view(-28,27)
grid
hold off

%% Plot Full Flight Profile
figure(3);
subplot(411);
```

```
plot(File(:,5),File(:,22),File(:,5),File(:,52))

title({'Full Altitude Profile';testsite;DateString});
ylabel('Altitude (m)');
legend('GPS Altitude','Baro Altitude','Location','Best')
axis tight

subplot(412);
plot(File(:,5),Acceltot)
title('Total Acceleration');
ylabel('a_{xyz} (m/s^2)');
axis tight

subplot(413);
plot(File(:,5),File(:,23))
title('GPS Ground Speed');
ylabel('Ground Speed (m/s)');
axis tight

subplot(414);
plot(File(:,5),File(:,24))
title('GPS Ground Track');
xlabel('Time (s)');
ylabel('Degrees (^o)');
axis tight

%% Create Plot of X-Monkey Roll, Pitch, and Yaw
figure(11)
subplot(311)
plot(SSDropProfile(:,5),eul(:,1))
title({'X-Monkey Euler Angles';testsite;DateString});
ylabel('\phi (^o)');
axis tight

subplot(312)
plot(SSDropProfile(:,5),eul(:,2))
ylabel('\theta (^o)');
axis tight

subplot(313)
plot(SSDropProfile(:,5),eul(:,3))
ylabel('\psi (^o)');
xlabel('Time (s)');
axis tight

%% Create Plot of Snowflake Roll, Pitch, and Yaw
figure(5)
subplot(311)
plot(SSDropProfile(:,5),SFeul(:,1))
title({'Snowflake Euler Angles';testsite;DateString});
ylabel('\phi (^o)');
axis tight

subplot(312)
plot(SSDropProfile(:,5),SFeul(:,2))
```

```
ylabel('\theta (^o)');
axis tight

subplot(313)
plot(SSDropProfile(:,5),SFeul(:,3))
ylabel('\psi (^o)');
xlabel('Time (s)');
axis tight

%% Create Euler Rate Plots
figure(6)
subplot(311)

frrate=medfilt1(-SSDropProfile(:,37),500);
fprate=medfilt1(-SSDropProfile(:,35),500);
fyrate=medfilt1(-SSDropProfile(:,36),500);

plot(SSDropProfile(:,5),-SSDropProfile(:,37))
hold on
plot(SSDropProfile(:,5),frrate,'r','LineWidth',2)
title({'Roll, Pitch and Yaw Rates';testsite;DateString});
ylabel('$\dot{\phi} (^o/s)$', 'Interpreter','latex')
axis tight

subplot(312)
plot(SSDropProfile(:,5),SSDropProfile(:,35))
plot(SSDropProfile(:,5),fprate,'r','LineWidth',2)
ylabel('$\dot{\theta} (^o/s)$', 'Interpreter','latex')
axis tight

subplot(313)
plot(SSDropProfile(:,5),-SSDropProfile(:,36))
plot(SSDropProfile(:,5),fyrate,'r','LineWidth',2)
ylabel('$\dot{\psi} (^o/s)$', 'Interpreter','latex')
xlabel('Time (s)');
axis tight

%% Create Acceleration Plots
figure(7)
subplot(311)
plot(SSDropProfile(:,5),SSDropProfile(:,34))
title({'Accelerations';testsite;DateString});
ylabel('a_{x} (m/s^2)');
axis tight

subplot(312)
plot(SSDropProfile(:,5),SSDropProfile(:,32))
ylabel('a_{y} (m/s^2)');
axis tight

subplot(313)
plot(SSDropProfile(:,5),SSDropProfile(:,33))
ylabel('a_{z} (m/s^2)');
xlabel('Time (s)');
axis tight
```

```
%% Create Control Input Plots
figure(8)
subplot(211)
hold on
plot(SSDropProfile(:,5),SSDropProfile(:,59),'Color','r')
hline0=refline(0,Servo0neutral);
set(hline0,'LineStyle','--');
title({'Control Line Inputs (Right)';testsite;DateString});
ylabel('Servo Zero Command (PWM)');
ylim([Servo0neutral-150 Servo0neutral+150]);
hold off

subplot(212)
hold on
plot(SSDropProfile(:,5),SSDropProfile(:,60),'Color','r')
hline1=refline(0,Servo1neutral);
set(hline1,'LineStyle','--');
title({'Control Line Inputs (Left)';testsite;DateString});
ylabel('Servo One Command (PWM)');
ylim([Servo1neutral-150 Servo1neutral+150]);
hold off

%% Compare Yaw Angle and Ground Track Plot
figure(9)
hold on
plot(SSDropProfile(:,5),SFeul(:,3))
plot(SSDropProfile(:,5),SSDropProfile(:,24))
title({'Yaw Angle vs GPS Ground Track';testsite;DateString});
ylabel('Yaw/Ground Track (^o)');
xlabel('Time (s)');
legend('Magnetometer Heading','GPS Ground Track')
axis tight
hold off

%% Three axis GPS velocity
figure(10)

hold on;
subplot(311)
hold on
plot(SSDropProfile(:,5),SSDropProfile(:,25))
plot(SSDropProfile(:,5),SSDropProfile(:,26),'--')
title({'GPS Velocity Data';testsite;DateString});
ylabel('V_{N;E} (m/s)');
legend('V_{N}','V_{E}','Location','best')
axis tight
hold off

subplot(312)
hold on
plot(SSDropProfile(:,5),SSDropProfile(:,27))
plot([SSDropProfile(1,5) SSDropProfile(end,5)]
,mean(SSDropProfile(:,27))*[1 1],'-.r');
text(SSDropProfile(1,5),mean(SSDropProfile(:,27)),['mean V_{D} = '
num2str(mean(SSDropProfile(:,27))) ' m/s']);
```

```
ylabel('V_{D} (m/s)');
axis tight
hold off

subplot(313)
VG=sqrt(SSDropProfile(:,25).^2+SSDropProfile(:,26).^2); mVG=mean(VG);
hold on
plot(SSDropProfile(:,5),VG)
plot([SSDropProfile(1,5) SSDropProfile(end,5)] ,mVG*[1 1],'-.r');
text(SSDropProfile(1,5),mVG,['mean V_{G} = ' num2str(mVG) ' m/s']);
ylabel('V_{G} (m/s)');
xlabel('Time (s)');
axis tight
hold off
```

LIST OF REFERENCES

Arcturus UAV. 2015a. "T-20." Accessed March 29, 2016. http://arcturus-uav.com/product/t-20.

——. 2015b. "JUMP 20." Accessed March 29, 2016. http://arcturus-uav.com/product/jump-20.

Barber, Justin, David Montague, and Larry Barello. 2011. "Use of Agile Methodologies to Develop Robust and Supportable Parachute Systems for the U. S. DOD." Paper presented at the 21st AIAA Aerodynamic Decelerator Systems Technology Conference and Seminar, Dublin, Ireland, May 23–26.

Benney, Richard, Justin Barber, Joseph McGrath, Jaclyn McHugh, Greg Noetscher, and Steve Tavan. 2005a. "The Joint Precision Airdrop System Advanced Concept Technology Demonstration." Paper presented at the 18th AIAA Aerodynamic Decelerator Systems Technology Conference and Seminar, Munich, Germany, May 24–26.

———. 2005b. "The New Military Applications of Precision Airdrop Systems." Paper presented at AIAA Infotech@Aerospace Conference, Arlington, Virginia, September 26–29.

Blanchard, Benjamin S., and Wolter J. Fabrycky. 2011. *Systems Engineering and Analysis*. Upper Saddle River, NJ: Prentice Hall.

Brown, Glen, and Richard Benney. 2005. "Precision Aerial Delivery Systems in a Tactical Environment." Paper presented at the 18th AIAA Aerodynamic Decelerator Systems Technology Conference and Seminar, Munich, Germany, May 24–26.

Hewgley, Charles W. 2014. "Pose and Wind Estimation for Autonomous Parafoils." Ph.D. diss., Naval Postgraduate School.

Defense Industry Daily. 2014. "JPADS: Making Precision Airdrop a Reality." Accessed on March 21, 2016. http://www.defenseindustrydaily.com/jpads-making-precision-airdrop-a-reality-0678/.

Lingard, Steven. 2015. "Basic Analysis of Ram-Air Parachute." In *Precision Aerial Delivery Systems: Modeling, Dynamics, and Control*, edited by Oleg A. Yakimenko. Reston, Virginia: American Institute of Aeronautics and Astronautics, Inc.

Office of Naval Research (ONR). 2012. “Autonomous Aerial Cargo/Utility System (AACUS) Innovative Naval Prototype (INP) Concept of Operations (CONOPS).” Accessed March 21, 2016. http://www.onr.navy.mil/~/media/Files/Funding-Announcements/BAA/2012/12-004-CONOPS.

United States Marine Corps (USMC). 2013. “Marine Corps Installations and Logistics Roadmap.” Accessed May 21, 2026. https://marinecorpsconceptsandprograms.com/sites/default/files/files/Marine%20Corps%20Installations%20and%20Logistics%20Roadmap.pdf

Yakimenko, Oleg A. 2015. “PADS and Measures of Their Effectiveness.” In *Precision Aerial Delivery Systems: Modeling, Dynamics, and Control*, edited by Oleg A. Yakimenko. Reston, Virginia: American Institute of Aeronautics and Astronautics, Inc.

Yakimenko, Oleg, Eugene Bourakov, Charles Hewgley, Nathan Slegers, Red Jensen, Andrew Robinson, Josh Malone, and Phil Heidt. 2011. “Autonomous Aerial Payload Delivery System ‘Blizzard.’” Paper presented at the 21st AIAA Aerodynamic Decelerator Systems Technology Conference and Seminar, Dublin, Ireland, May 23–26.

INITIAL DISTRIBUTION LIST

1. Defense Technical Information Center
   Ft. Belvoir, Virginia

2. Dudley Knox Library
   Naval Postgraduate School
   Monterey, California